Interreg North Sea

Co-funded by the European Union

WaterWarmth

Interreg North Sea

Co-funded by the European Union

WaterWarmth

Workpackage 4

Smart integration of AE in the local energy system

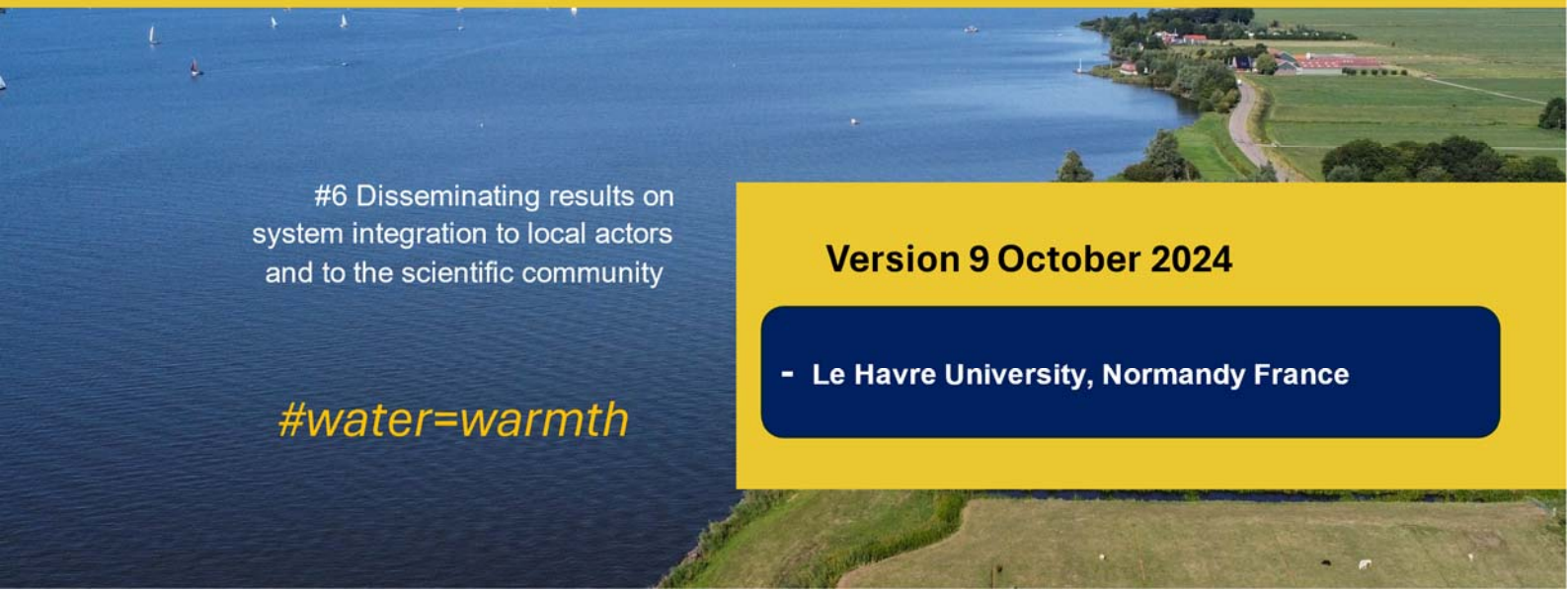

#6 Disseminating results on system integration to local actors and to the scientific community

#water=warmth

Version 9 October 2024

- **Le Havre University, Normandy France**

A GREEN TRANSITION

WATER = WARMTH

electronics

MDPI

Review

Power Converter Topologies for Heat Pumps Powered by Renewable Energy Sources: A Literature Review

Joyce Assaf *, Joselyn Stephane Menye *, Mamadou Baïlo Camara, Damien Guilbert and Brayima Dakyo

Laboratoire Groupe de Recherche en Electrotechnique et Automatique du Havre (GREAH), Université le Havre Normandie (ULHN), 76600 Le Havre, France; camaram@univ-lehavre.fr (M.B.C.); damien.guilbert@univ-lehavre.fr (D.G.); brayima.dakyo@univ-lehavre.fr (B.D.)

* Correspondence: joyce.assaf@univ-lehavre.fr (J.A.); joselyn-stephane.menye@etu.univ-lehavre.fr (J.S.M.)

Abstract: Heat pumps (HPs) have become pivotal for heating and cooling applications, serving as sustainable energy solutions. Coupled with renewable energy sources (RES) to run the compressor, which is the major energy-consuming component, they contribute to eco-conscious practices. Notably, their adaptability to be supplied by either alternating (AC) or direct (DC) currents, facilitated through converters, makes them more flexible for versatile renewable energy (RE) applications. This paper presents a comprehensive review of converter topologies employed in various HP applications. The review begins by exploring previous applied photovoltaic (PV)-HP projects, focusing on the gaps in the literature concerning the employed converter topologies. Additionally, the review extends to include a broader examination of the converter topologies that could be employed on the source and load sides of a system powered by a mix of renewable energy sources, such as photovoltaics (PV), wind turbines (WTs), and energy storage systems (ESS), and analyzes their strengths and weaknesses. Special emphasis is given to understanding the various topologies of the power electronics converters in the context of HP applications. Finally, the paper concludes with a summary of the literature gaps, challenges, and directions for future research.

Keywords: heat pumps; renewable energy; converter topologies; DC-driven heat pump; AC-driven heat pump; DC-DC converters; AC-DC converters; DC-AC converters

Citation: Assaf, J.; Menye, J.S.; Camara, M.B.; Guilbert, D.; Dakyo, B. Power Converter Topologies for Heat Pumps Powered by Renewable Energy Sources: A Literature Review. *Electronics* **2024**, *13*, 3965. https://doi.org/10.3390/electronics13193965

Academic Editors: Antonio J. Marques Cardoso, Fernando Bento and Khaled Laadjal

Received: 27 August 2024
Revised: 1 October 2024
Accepted: 3 October 2024
Published: 9 October 2024

1. Introduction

In Europe, heating and cooling account for almost 50% of its total gross final energy consumption [1]. The residential sector has gained particular interest as nearly 64% of the final energy consumption was attributed to heating households in 2021, out of which renewables accounted for only 27% [2,3]. According to the International Energy Agency, around 25% of the world's total energy consumption in 2021 was allocated to space heating and domestic hot water [2]. This share could significantly increase especially in countries with colder climates [4], emphasizing the imperative need for the development and adoption of more efficient and carbon-neutral heating and cooling systems [5].

In a collective endeavor to reach the net zero emission goals by 2050, heat pumps (HPs) are now the most promising technology to decarbonize the energy sector while promoting renewable energy (RE) integration [6], due to their high thermodynamic efficiency and the possibility of using electricity from RE as a source. A HP is a device which extracts heat from a low-temperature renewable energy source (RES) such as air (air-source heat pump (ASHP)), ground (ground-source heat pump (GSHP)), or water (water-source heat pump (WSHP)), or from processed waste such as wastewater, and transfers it to a warmer or high-temperature place, also known as a heat sink, by means of a refrigeration cycle [7].

In recent years, the role of HPs in the energy system has been influenced by the notable rise in RE generation from wind turbine (WT) and photovoltaic (PV) plants [8,9].

In Germany, for instance, the government has set a target to install 500,000 HPs, starting in 2024, with heating systems in buildings operating with at least 65% RE [10]. The coupling of heating and electricity systems, as in the case of PV-HPs, for example, has been attracting broad interest [10]. This coupling is carried out through converters. However, the efficiency of these systems is heavily influenced by the way in which the RES power is extracted and converted [11]. Typically, RES and energy storage systems (ESSs) are connected to the grid through converters [12]. The converter serves as the primary component in power electronics systems, enabling voltage to be either increased or decreased [13], and ensures stable interfaces between the source and load sides [14].

Electrically driven HPs are used for space heating as well as the production of domestic hot water [15]. The compressor of RE-driven HPs can be powered by either DC or AC. While AC-powered HPs require a DC-to-AC inverter for RE integration, DC-powered HPs can be coupled with some RES, such as PV systems, through DC-DC converters. Power electronics converters are classified into four categories [16–18]:

- AC-DC converters—also called rectifiers—which are used in household appliances, cellular phones, and laptops.
- DC-AC converters, which are used in grid-connected RES such as solar PV, WT, and motor drives.
- DC-DC converters, which convert DC input voltage from one level to another. They are used in ESS to maximize the energy harvested by RES such as PVs or WTs. Some other applications include electric vehicles.
- AC-AC converters, which convert AC voltage at one frequency to AC voltage at another frequency or alter the amplitude of AC voltage.

A hybrid system combines two or more energy sources, such as PV, WT, and ESS or grid-tied PV-WT, to complement each other and meet energy demands efficiently [19]. The hybrid-system-based DC-bus configuration is the least restrictive in terms of coupling various sources and the most flexible in terms of energy management [20]. As shown in Figure 1, the outputs from the WT, PV array, and ESS are connected to the DC-bus through an AC-DC converter, a DC-DC converter, and a bidirectional converter (BDC), respectively. A DC-AC converter is required when an AC load needs to be supplied.

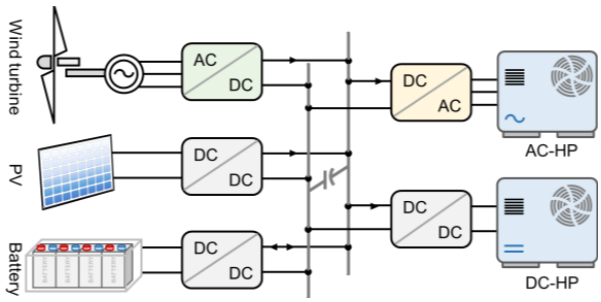

Figure 1. Configuration of a hybrid system integrating a battery ESS.

A wide range of studies has focused on developing new converter topologies to overcome the challenges faced by conventional designs, propose new design requirements, and address real-world constraints. However, the literature lacks information regarding converter topologies specifically used for HP systems powered by RES such as PV and/or WT with or without an ESS. Thus, this study aims to provide a structured overview of the different topologies of DC-DC, AC-DC, and DC-AC converters considering an energy mix on the source side, such as PVs and/or WTs and/or an ESS, and the HP on the load side. The goal is to offer researchers a comprehensive introduction to the topic, along with a summary of findings, structure, and guidance for future research.

The paper is organized as follows: Section 2 provides an overview of various studies in the literature discussing HPs powered by RES, primarily PV systems. Section 3 details the converter topologies that could be used in DC-powered HP systems, along with existing

topologies and the associated challenges. Section 4 focuses on the converter topologies that could be used in AC-powered HP systems, including existing topologies and their challenges. Finally, Section 5 concludes the article with directions for future research.

2. Overview of Previous RE-Powered Heat Pumps Applications

The concept of integrating HPs in the smart grid, combined with RES such as PVs or WTs, as the two main fast-growing sources of fluctuating renewable electricity generation, has gained increasing attention [9]. One of the most important objectives of this combination, other than providing efficient heating and cooling solutions, is to maximize the use of RE through the HP's electricity consumption, and adjusting their operation to match energy availability [21,22]. For instance, the synergy between cooling demand and PV electricity generation is particularly evident during hot periods when both demand and production reach their highest levels [23].

Nevertheless, research into HP systems powered by RES is still in its early stages. Most of the studies found in the literature report experimental or simulation results for grid-connected systems or a stand-alone PV-HP, with no emphasis on the used converter topologies. Rieck et al. [24] proposed a system including a HP (11–14 kW) powered by PVs, a WT, and the grid. However, this techno-economic study consists of simulations without specifying the converter topology used.

The first simulation study was conducted in 2011 in Serbia, where Bojić et al. [25] investigated the energy consumption of a PV AC-driven WSHP (14 kW) system in residential houses for different PV system sizes. Similarly, Roselli et al. [26] simulated the operation of a PV (4.5, 6, 7.5 kW) AC-driven ASHP (4.12–4.22 kW). Klokov et al. [27] evaluated various design approaches for a PV (47 kW) powering two AC-driven HPs (3.25 kW each) for thermal stabilization of a 100 m^2 area in northern Norway.

Other research works consisted of experimental studies. For instance, Izquierdo et al. [28] assessed the performance of a PV (2.9 kW) AC-driven ASHP system with a 250 Ah ESS for a laboratory prototype in Spain, while Franco and Fantozzi [29] analyzed the level of interaction of a PV (3.7 kW) GSHP (3.8 kW) system with the grid for a house in Italy. Aguilar et al. [30,31] reported a full year's operation of a PV (0.705 kWp) HP (0.86–0.99 kW) in a standard 35 m^2 office in Alicante, southeast Spain. The DC-driven HP was powered simultaneously by PVs through a solar control converter and the grid through a frequency converter. The direct integration of the solar PV panels into the inverter HP lowered the grid consumption throughout the year, with the PVs producing 70% of their potential electricity output and contributing in total to 53.8% of the AC unit's electricity consumption. In [32], the authors proposed an innovative system featuring a 5 kWp PV system, a 10 kW DC/AC BDC for the 45 Ah ESS, and a 13 kW cooling capacity DC-driven HP. The DC-driven HP directly consumes the electric energy generated by the PV system via a DC-DC converter. However, no information on the topology is provided except that the converter is bidirectional.

Other works in the literature were based on field measurement data. For instance, in [10], the authors investigated the performance of a smart-grid-ready controlled PV (12.3 kWp) AC-driven GSHP (13.9 kW) system aided by a 11.7 kWh ESS, in Freiburg, Germany. The AC-converter-driven smart-grid-ready interface optimized HP operation for increased PV self-consumption.

However, in all the aforementioned research works, results were based on simulations without indication of the used converter topologies. In [33], the authors proposed a high-voltage-gain DC-DC converter (shown in Figure 2) specifically tailored for a 76 kW PV system powering a 55 kW HP. Their simulations, conducted under real weather conditions, demonstrated that, for a duty cycle of 0.5, the voltage gain of the proposed converter was four times higher than that of the conventional boost converter.

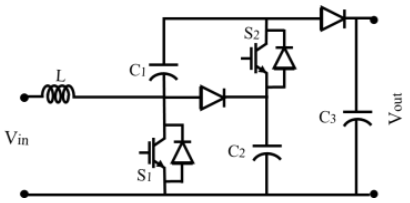

Figure 2. High-voltage-gain DC-DC converter.

Despite the progress detailed above, the significant gaps in the literature highlight the need for further investigation into optimal converter topologies to be integrated with the energy mix and their impact on system efficiency, reliability, and cost effectiveness. Addressing these gaps is essential for enhancing system efficiency and maximizing RE utilization, thereby fueling the smart integration of RES into HP systems in order to drive sustainable heating and cooling solutions.

3. Converter Topologies for DC-Powered HPs

3.1. Unidirectional DC-DC Converter Topologies on the PV Side or DC-Powered HP Side

Researchers have shown a growing interest in DC-driven HPs in recent years [34]. In fact, the concept of DC and hybrid AC/DC systems has gained more interest as the penetration of RES in DC electricity generation has risen as well as the number of residential loads that are DC-powered [32]. Green energy technologies enable direct powering of DC compressors, whereas AC compressors require power inverters [35]. DC-motor-driven HP technologies designed for water and space heating can surpass conventional resistance heating methods, achieving savings exceeding 50% in energy consumption [36]. On the other hand, AC compressors operate on alternating voltage, 120 or 220 V and 50 or 60 Hz, while DC compressors operate on a low-voltage supply of 12–24 V [35].

High-step-up DC-DC converters are widely used in RE systems, to meet the DC line voltage requirements [37–39], due to the variable and low-output voltage generated by RES such as PVs and WTs. In fact, the electric power generated by the common RES is in the range of 12–70 VDC, and needs to be boosted to 200–400 VDC [40]. Nowadays, the challenge lies in designing topologies that simultaneously achieve low cost, low weight, reduced switching voltage stress, and high power density [41]. High-step-up DC-DC converters can be categorized as isolated or non-isolated [39,42]. In PV applications, conventional non-isolated converters like boost [43], buck–boost [44], cuk [45], sepic [45], and zeta converters [46] have limited voltage gain [47], and thus are not suitable for high-voltage/power applications [39,48,49]. These topologies are depicted in Figure 3.

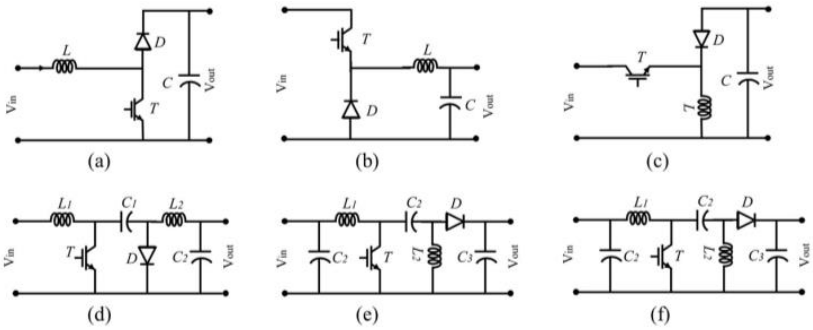

Figure 3. (**a**) Boost (**b**) buck (**c**) buck–boost (**d**) cuk (**e**) sepic, and (**f**) zeta high-step-up DC-DC converter topologies.

A boost converter is a step-up converter that produces an output voltage higher than the input voltage [16]. Although it benefits from the minimum component stresses for a given voltage conversion ratio [50], the classic boost converter topology has limited voltage gain due to the parasitic elements of inductors, capacitors, and switching semiconduc-

tors [51]. However, in high-power applications, such basic topologies are subject to voltage stress constraints on the power components. As a solution, multilevel DC-DC converters have been proposed in the literature. By dividing the overall voltage conversion into smaller steps and distributing the voltage and current loads across multiple levels, they ensure the reliability and durability of the power components.

Emerging technologies require alternative configurations where the voltage conversion ratio is dependent on the duty cycle [52]. Due to the current imbalance caused by the integration of the PV panels into the grid [53], there has been a growing preference for employing isolated step-up DC-DC converters in PV applications, largely driven by the safety benefits offered by isolation [54]. Isolated converters such as dual-half-bridge (DHB), dual-active-bridge (DAB), half-bridge, full-bridge, flyback, and push–pull converters are suitable for high-voltage/power applications [39]. They are typically used in applications where galvanic isolation between high and low voltages is required, achieved through high-frequency transformers, whereas non-isolated converters are used in applications where the galvanic electric separation between the load and the source is not required. Thus, isolated converters are complex and bulky because they use special transformers while non-isolated converters are simpler and smaller [55].

Moreover, various methods were introduced to improve voltage gain, including switched capacitors, voltage multipliers (comprising voltage multiplier cells (VMC) and voltage multiplier rectifiers), magnetic-coupling-based techniques, tapped inductor designs, isolated and integrated transformers, and multi-stage approaches like interleaved, multilevel, and cascaded (including hybrid and quadratic) configurations [56].

Quadratic converters feature voltage conversion ratios that depend on the square of the duty cycle and are two-stage converters formed of two cascaded converters [52]. A single-switch high-step-up Y-source boost converter was proposed in [57] to overcome challenges related to high voltage stress on the switches [58,59] and discontinuous input current [60,61]. Although the laboratory prototype of the proposed converter achieved a maximum efficiency of 95% at 300 W and 100 kHz, the topology was notably complex.

In [62], a non-isolated high-step-up DC-DC converter designed for grid-tied PV systems was introduced, featuring dual coupled inductors and a parallel input connection to share current and reduce ripple. A 1 kW laboratory prototype proved the converter to be 93.6% efficient at full load, achieving a high voltage gain (30–400 V). Key advantages included its ability to handle high-voltage step-up ratios and power levels due to the dual inductor and shared current design. Additionally, it minimized ripple current at the input through small magnetizing inductors, implemented low ON-state resistance switches to reduce voltage stress, and operated with zero voltage switching (ZVS) for switches and zero current switching (ZCS) for diodes, effectively minimizing switching losses. Moreover, integrated regenerative snubber and clamp circuits eliminated turn-off voltage spikes and ringing on switches caused by leakage inductance, ensuring efficient and reliable performance.

A soft-switched non-isolated high-step-up DC-DC converter utilizing coupled-inductor and voltage multiplier cell techniques was introduced in [63]. It offered several advantages, including continuous input current with low ripple, low voltage stress on semiconductors, soft switching of diodes, high voltage gain, compact size, low cost, and high power efficiency. Despite achieving outstanding efficiency across different output powers and input voltages (25 V, 30 V, and 33 V), with a peak efficiency of 97% at 120 W output power (Vin = 33 V), the proposed topology suffered from pulsating input current.

In [64], a novel non-isolated high-voltage-gain DC-DC converter for PV applications was introduced. It used a small-sized coupled inductor to enhance the voltage conversion ratio and featured a single active MOSFET with low conduction resistance to minimize leakage and simplify control complexity. An experimental prototype was built with a 20 V input, a 200 V output, a power rating of 200 W, and a converter operating frequency of 50 kHz to validate the mathematical analysis and effectiveness of the proposed structure. The efficiency of the proposed converter was estimated to be approximately 96% at 200 W.

In [65], the authors proposed a novel non-isolated cubic high-gain DC-DC converter based on the traditional quadratic DC-DC boost converter by incorporating a switched-inductor–capacitor unit to address challenges related to the low output voltage generated by renewables. The experimental prototype operated with an input voltage of 12 V, generated an output voltage of 72.9 V, and achieved a power output of 57 W at full load. It reached a 92% conversion efficiency with high voltage gain and low device stress, compared to the traditional quadratic boost converter, which utilizes a single switch with high voltage and current ratings, resulting in decreased efficiency at higher duty ratios [37].

In [66], a step-up LC resonant converter (RC) was proposed for a grid-connected RES with the purpose of reducing switching losses and voltage stress on the semiconductor devices and achieving high voltage gain. A 100 V (±20%)/1000 V, 1 kW prototype was built, demonstrating its suitability for high-power, high-voltage applications. However, there is no guarantee of the reliability of the resonant inductor and capacitors under continuous high-power operation.

The DC-DC converter proposed in [67] represented a significant advancement in PV system integration by achieving a high step-up voltage conversion ratio and integrating a model predictive control (MPC) algorithm optimized for PV applications. With the capability to increase the input voltage up to ten times, from 20 V to 100 V DC, the converter efficiently harvested power from the PV panels under varying environmental conditions. The accompanying MPPT algorithm ensured optimal operation by using an ideal number of sensors, balancing system complexity with performance. However, despite achieving an impressive 93% efficiency, which is suitable for many PV applications, it fell slightly short of the 95% efficiency threshold often required for optimal PV integration according to industry standards. Moreover, its scalability and suitability for higher voltage levels beyond 100 V DC remain areas of consideration, potentially limiting its application in larger-scale PV systems without further enhancements or modifications.

In [68], the authors proposed an ultra-high-gain quadratic DC-DC boost converter that achieved a voltage gain with an efficiency of 90% and a low duty cycle. However, it required two separate control power supplies due to the use of two semiconductor switches without a common ground, which increased the system's cost and complexity.

Table 1 summarizes the aforementioned non-isolated converter topologies, along with their specific characteristics.

In [69], the authors built a 288 W prototype of an isolated soft-switching current-fed LCC-T resonant DC-DC converter for PV applications, which resolved challenges such as achieving high voltage gain, reducing switching losses, and ensuring continuous input current with minimal ripple. However, the necessity for frequency modulation resulted in component designs at a lower frequency (175 kHz), making them 17% oversized compared to components designed for higher frequencies (210 kHz), which potentially leads to higher costs. In [70], the authors proposed a switched coupled inductor boost to overcome excessive conduction and switching losses. Despite achieving impressive efficiencies of 97%, 98%, and 99% at output powers of 250 W, 200 W, and 150 W, respectively, with an input voltage of 50 V, a duty cycle of 0.7, and an output voltage of 500 V, the proposed converter suffered from pulsating input current and the absence of a common ground connection.

Table 1. Non-isolated DC-DC converters on the PV side.

Topology	Name	Voltage Gain	Efficiency	Advantages	Disadvantages	Experimental Prototype
[57]	Single-switch high-step-up Y-source boost converter	$\frac{2+N}{[1-D(1+m)]}$ $(1-D)$	95%	Maintains good trade-off between high voltage gain and low voltage stress of the devices.	Requires two separate control power supplies, which increases system cost and complexity.	300 W 48 V DC input 380 V DC output
[62]	High-efficiency high-step-up DC-DC converter with dual coupled inductors for grid-connected PV systems	$\frac{2(N+1)}{1-D}$	94%	• Can handle high power levels due to its dual coupled inductor design and shared input current structure. • Low ripple current at the input. • Reduced conduction losses. • Minimized switching losses. • Turn-off voltage spikes eliminated due to integrated regenerative snubber and clamp circuits.	• Complex design due to the integration of active clamp circuits, regenerative snubbers, and dual coupled inductors. • Higher cost.	1 kW 30 V DC input 400 V DC output
[63]	Soft-switched high-step-up DC-DC converter utilizing coupled inductor and voltage multiplier cells	$\frac{2+3N}{1-D}$	95%	• Continuous input current with low ripple. • Low voltage stress across semiconductors. • Soft switching of diodes (ZVS and ZCS). • High voltage gains with low duty cycle. • Low volume and cost. • High power efficiency.	• Pulsating input current. • Lack of common ground connection.	200 W 33 V DC input 403 V DC output
[64]	Novel high-gain soft-switching DC-DC converter with improved P&O MPPT	$\frac{2N-1}{(1-D)(N-1)}$	96%	• Uses a small-sized coupled inductor to enhance the voltage conversion ratio. • Features a single active MOSFET with low conduction resistance to minimize leakage. • Low input current ripple. • High efficiency. • Simple structure. • Peak voltage throughout the semiconductor components. • Low component count. • Simplified control complexity.	• Low efficiency for medium- and high-power applications. • Less reliable in case of failure of the single power switch.	200 W 20 V DC input 200 V DC output

Table 1. *Cont.*

Topology	Name	Voltage Gain	Efficiency	Advantages	Disadvantages	Experimental Prototype
[65]	Cubic high gain	$\frac{1+(1-D)^2}{(1-D)^3}$	92%	• Reduces switching losses. • Ensures continuous input current with minimum ripples.	Necessitates frequency modulation, which results in the design of components at a lower frequency (175 kHz), making them 16.66% oversized compared to components designed for higher frequencies (210 kHz), which potentially leads to higher costs.	57 W 12 V DC input 75.5 V DC output
[66]	Step-up LC RC	Dependent on the parameters of the resonant tank (Lr and Cr)	95%	• Minimizes voltage imbalances. • Allows operation at any gain value (>2) with proper control.	• Exhibits efficiency decrease at lower output power due to increased switching losses. • Higher input voltages lead to higher switching frequencies and increased switching losses.	1 kW 100 V DC input 1000 V DC output
[67]	A new high-gain DC-DC converter with MPC-based MPPT for PV system	$\frac{1+D}{1-D}$	93%	• Demonstrates superior performance over transformer-less counterparts in terms of efficiency, reliability, and cost effectiveness. • Overcomes limitations of transformer-less designs such as insulation requirements, leakage current issues, and safety concerns in grid-connected PV systems.	• Efficiency is less than 95%, which is required for PV integration [64]. • Might be unsuitable or not scalable for higher voltage levels.	150 W 20 V DC input 100 V DC output
[68]	Ultra-high-gain quadratic DC-DC boost converter	$\frac{3-D}{(1-D)^2}$	90%	• Achieves exceptionally high-level of voltage gain with a low duty cycle. • Reduced voltage stresses on devices.	Requires two separate control power supplies due to the presence of two semiconductor switches without a common ground, which increases system cost and complexity.	150 W 12 V DC input 80 V DC output

In all the voltage gain formulas that follow, the term 'D' represents the duty cycle, while 'N' denotes the turns ratio, which is the ratio of the number of turns in the primary winding to those in the secondary winding of a transformer.

In [71], the authors proposed a dual-flyback DC-DC converter with a resonant voltage multiplier, addressing challenges related to the high turns ratio, which leads to increased transformer size, surge voltage caused by leakage inductor of the transformer, and conduction losses. The prototype operated with an input voltage range of 24 V, providing an output voltage of 200 V at a maximum power of 120 W, with a switching frequency of 50 kHz. It demonstrated 96.5% efficiency for output powers ranging from 40 to 60 W and achieved a higher voltage gain than the traditional flyback converter; however, the topology remains complex. In [72], a flyback converter utilizing a voltage doubler circuit was proposed to boost output voltage with fewer turns, addressing challenges associated with the high turn ratio of conventional flyback converters that lead to increased current stresses on the switches. The 200 W prototype, operating at a switching frequency of 50 kHz and producing an output voltage of 350 V, achieved a peak efficiency of up to 96% at a power output of 125 W. In [73], the authors proposed a flyback converter with an active clamp circuit that recovers the leakage energy of the flyback transformer and charges a clamping capacitor using the trapped leakage energy. The prototype converter operates with an input voltage range of 18 V to 22 V, delivering a steady output voltage of 110 V with a maximum power output of 40 W while operating at a high switching frequency of 100 kHz and with a duty ratio limited to 0.5. However, the prototype's efficiency was 86% at various loading conditions and at full load.

In [74], a novel DC-DC converter with high current capability was introduced to address current technical limitations by introducing three key innovations: parallel operation, direct transmission of partial power, and non-AC energy balancing. However, the experimental prototype experienced more voltage variations and current fluctuations than predicted in the simulations, which suggests that the converter may have difficulty maintaining consistent performance.

In [75], the authors proposed a novel self-reconfigurable LLC-type resonant converter that achieved an efficiency of 95%. It offered high voltage gain while maintaining low switch losses and reducing voltage stress on the switches. However, it experienced discontinuous current flows, which can negatively impact the performance of RES and battery efficiency.

Table 2 summarizes the aforementioned isolated converter topologies, along with their specific characteristics.

Table 2. Isolated DC-DC converters on the PV side.

Topology	Name	Efficiency	Advantages	Disadvantages	Experimental Prototype
[69]	Soft-switching current-fed LCC-T resonant	95%	• Reduces switching losses and voltage stress on the semiconductor devices. • Ensures continuous input current with minimum ripples.	There is no guarantee of the reliability of the resonant inductor and capacitors under continuous high-power applications.	288 W 30–42 V DC input 380 V DC output
[70]	Switched coupled inductor boost	97%	• Uses only one magnetic element, so the design is simple. • The active switch inductor cells have tightly coupled inductors, minimizing issues caused by mismatches between inductors.	• Pulsating input current. • Lack of common ground connection. • Complexity in implementation.	250 W 50 V DC input 500 V DC output
[71]	Dual-flyback DC-DC converter with a resonant voltage multiplier	96.5%	• No need for snubber/clamping circuits. • Reduced voltage stress on diodes.	• Complex topology. • Potential for resonance issue.	120 W 24 V DC input 200 V DC output

Table 2. *Cont.*

Topology	Name	Efficiency	Advantages	Disadvantages	Experimental Prototype
[72]	Flyback converter utilizing a voltage doubler circuit	96%	• Boosts output voltage with fewer turns. • Decreased current stress on the switches.	• Complex control algorithms. • Advanced control techniques and circuit configurations may be more sensitive to variations in component parameters, which could affect the converter's reliability and performance consistency.	125 W 24 V DC input 350 V DC output
[73]	Flyback converter with an active clamp circuit	86%	Recovers the leakage energy of the flyback transformer and charges the clamping capacitor using the trapped leakage energy.	Low efficiency at various load conditions and at full load.	40 W 18–22 V DC input 110 V DC output
[74]	Novel DC-DC converter with high current capability	-	• Parallel operation facilitating the sharing of medium-voltage current across multiple strings of submodules, resulting in high current capability. • Direct transmission of partial power and non-AC energy balancing, reducing the number of cascaded submodules needed. • Higher efficiency. • Compact design (lower number of IGBT and capacitors).	The experimental prototype experienced more voltage variations and current fluctuations than predicted in the simulation, which suggests that the converter may have difficulty maintaining consistent performance.	1.2 kW 100 V DC input 300 V DC output
[75]	Novel self-reconfigurable LLC-type RC	95%	Achieves high voltage gain while maintaining low switch losses and reducing voltage stress on the switches.	Encountered discontinuous current flows impacting RES performance and battery efficiency.	300 W 25–50 V DC input 400 V DC output

3.2. Bidirectional DC-DC Converter Topologies on the ESS Side

Due to the intermittent nature of RES, such as PVs and WTs, ESSs are employed to compensate fluctuations between electricity generation and load demand. Power fluctuation imposes significant challenges on the power grid, including issues with power quality, load leveling, and generation dispatch control [76]. Thus, ESSs are integrated with RES to ensure the reliability and stability of the system by regulating the frequency and voltage, smooth the DC-bus voltage waveform and output power, and improve the system's dynamic response [77]. Among the various types of ESS available on the market, batteries and supercapacitors are the most frequently utilized components.

BDCs are pivotal components in modern RE systems, enabling power flow in both directions. They facilitate energy management for storing excess energy generated by RES during peak times through an ESS and retrieving it during periods of low production and high demand, thereby maximizing the utilization of RES, stabilizing the grid, and ensuring a consistent and reliable power supply. In the context of HPs, only a limited number of studies describe stand-alone installations that use an ESS [8].

BDCs are either isolated or non-isolated [78]. Non-isolated BDCs are more efficient for low-power applications due to their ease of control and lightweight design [79]. The classical non-isolated BDC is typically derived from the basic unidirectional converter topology illustrated in Figure 4a. The bidirectionality is achieved by creating a return path for current through the addition or modification of power components. For example, in a unidirectional boost converter, substituting the diode and IGBT with IGBT modules allows current to flow in the reverse direction, as illustrated in Figure 4b, thereby enabling bidirectional power flow. Similarly, in a buck converter, adding a switch in place of the input diode can achieve the same effect. The control strategy must also be updated to

handle power flow in both directions by adjusting the switching based on current directions. Other examples of non-isolated bidirectional cuk, sepic, switched-capacitor, and interleaved converters were explored in the literature, in [80–83] respectively. Similarly, examples of isolated bidirectional DHB, DAB, half-bridge full-bridge, flyback, and push–pull converters can be found in [84–90], respectively.

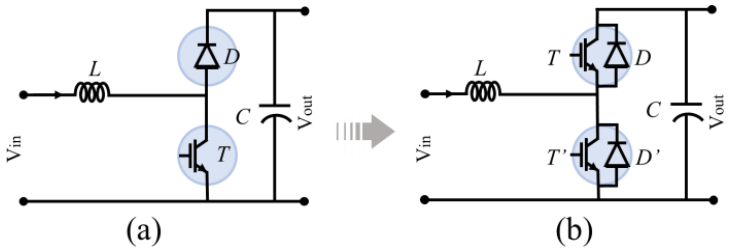

Figure 4. (**a**) Unidirectional boost converter and (**b**) bidirectional boost converter.

Additionally, incorporating a return circuit ensures continuous current paths for both charging and discharging modes. This is achieved by designing the converter with symmetrical components, as seen in a bidirectional buck–boost converter [91], where the boost mode is used during the battery's discharge stage to regulate the DC-bus voltage, while the buck mode is employed during the battery's charge stage. An example of a complex bidirectional converter is the DAB converter, which uses active switches on both the primary and secondary sides of a transformer to enable power transfer in both directions.

Bidirectionality can also be achieved through RCs. The RC is obtained by adding a resonant circuit to the basic DAB converter topology to enhance its efficiency [92]. Conventional RCs are classified as phase shift modulated and load resonant [93]. Load RCs are suitable for high-voltage applications due to their ability to operate at high frequencies, which significantly reduces the size of passive components and overall equipment without compromising power conversion efficiency [78].

RCs are employed to mitigate several key challenges faced by traditional hard-switching converters, such as high switching losses, reduced efficiency, excessive heat generation, and increased electromagnetic interference [94,95]. In addition to providing galvanic isolation, RCs offer a wide range of soft-switching options, such as ZVS or ZCS [96], and reduce output filter requirements. RCs are classified as two-element (series or parallel), three-element (LCC, LLC), and multi-element (CLLC) [97]. These topologies are illustrated in Figure 5. The voltage gain of LLC converters can be extended over a broad range by adjusting the inductance ratio and the switching frequency relative to the resonant frequency, allowing for great flexibility in controlling the output voltage. However, due to the nonlinearities introduced by the resonant network within these converters, their design and the implementation of a control strategy remain relatively complex.

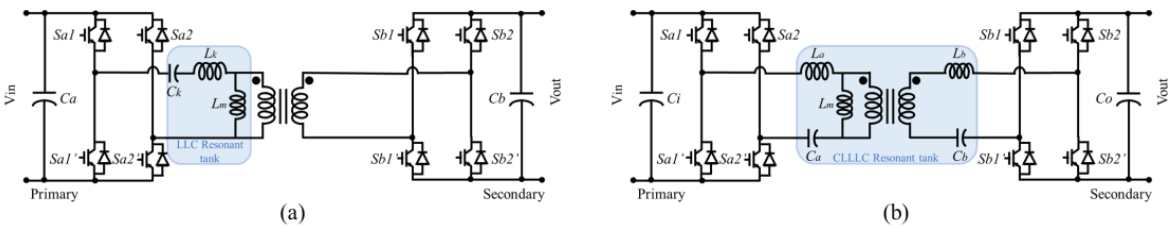

Figure 5. (**a**) LLC bidirectional RC and (**b**) CLLC bidirectional RC topologies.

LLC and CLLC are the most popular among bidirectional RCs and new topologies are derived from these basic configurations [98]. Many modified LLC topologies have been introduced in the literature [99–101]. In [102], a new bidirectional LLC RC topology was proposed that enables bidirectional current operation for an ESS, maintains precise switching frequency control across forward and backward operations, limiting turn-off

losses, and has a soft start mechanism at the resonant frequency. Additionally, it can operate under a wide voltage range of 60–240 V. A laboratory test bench integrating a 3 kW resonant circuit into a 12 kW DAB converter achieved a maximum efficiency of about 96% with a 240 V DC voltage source.

When the primary and/or secondary converter is of the multilevel type, it is referred to as a multilevel bidirectional RC. While it may face more complex control due to an increased number of semiconductors and capacitors, multilevel inverters (MLIs) offer several advantages, such as reduced voltage stress, lower losses in individual semiconductors, and improved energy efficiency. Research has focused on integrating multilevel configurations into isolated DC-DC conversions. For example, the three-level CLLC RC [103] can adapt to a wide voltage range, from 200 V to 700 V, by adding CLLC resonant components and combining the operating modes of two three-level inverters. Furthermore, ref. [104] explored the primary side phase leg topology for a multilevel DC-DC converter used in a solid-state transformer.

The advantages and disadvantages of the basic DC-DC converter topologies are given in Table 3. Specific emphasis is placed on comparing these topologies within the context of high-power applications for HPs. In accordance with the principle illustrated in Figure 4, different types of basic converters mentioned in Table 3 have their equivalents in terms of BDCs.

Table 3. Comparison of the basic isolated and non-isolated unidirectional/bidirectional high-step-up converter topologies.

Isolated/ Non-Isolated	Topology	Voltage Gain	Advantages	Disadvantages	Major Applications
Non-isolated	Buck and boost [43,44,105,106]	D and $\frac{1}{1-D}$	• Basic topology with noteworthy effectiveness • Wide range of input voltage	Higher electromagnetic interference	PV systems, with or without ESS
	Buck–boost [43,44,105,106]	$-\frac{D}{1-D}$			
	Sepic–zeta [45,46,107]	$\frac{D}{1-D}$	• Reduced ripple currents • Increased voltage gain	• Reduced efficiency because of the coupled inductors • Operating power range is limited • High voltage stress on the switch	ESS, distributed power systems
	Cuk [16,45,108,109]	$\frac{-D}{1-D}$	• Less ripple output current • Low cost as it has lower components • Could be operational in isolated state	Limited voltage gain	DC microgrid and integration between low-voltage high-current source and energy storage devices
	Cascaded [78,110–112]	$\frac{1}{1-D}$	• Reduced current ripples • High conversion efficiency because it utilizes only one inductor	High number of switches, which increases system cost and complexity	PV systems, ESS
	Switched capacitor [113–115]	2	• Reduced electromagnetic interference	• High-current transients, which have a degrading effect on both power density and efficiency • High output ripple current	PV systems, battery-powered systems, integrated circuits
	Interleaved boost [116]	$\frac{1}{1-D}$	• Reduced output current ripples • Reduced conduction losses • Fewer switches • Suitable for high-power applications	• High cost • Complex control techniques	ESS

Table 3. *Cont.*

Isolated/ Non-Isolated	Topology	Voltage Gain	Advantages	Disadvantages	Major Applications
Isolated	DAB [97,117,118]	-	• Very efficient in high-power applications • High conversion efficiency • Suitable for high-power applications	Complex control algorithms to manage the phase shift between the bridges	PV systems, ESS, hybrid energy systems, and DC microgrids
	Half-bridge [39,78,97,108,119]	DN	• Minimized switching losses • Low ripples • Wide operational input voltage range	Suitable for low-power applications	Residential PV systems
	Full bridge [39,78,97,108,119]	2DN	Suitable for high-power applications	• Larger number of components, which leads to higher cost • Complex structure and control	Industrial applications
	Flyback [39,78,97,119,120]	$\frac{DN}{1-D}$	• Cost effective for low-power applications • Leakage energy harvesting	• Limited output voltage • Suitable for low-power applications	PV systems, DC microgrids, distributed generation system
	Forward [39,78,97,119–121]	DN	• Suitable for medium-to-high-power applications • Minimized switching losses	Complex structure	PV systems
	Push–pull [122,123]	DN	• Steady current flow • Reduced weight and size • High efficiency and voltage gain	• When employed with PV, no maximum utilization of available solar energy • Complex structure and control	Grid-tied PV systems, ESS

In hybrid applications, the usage of multiport step-up converters is usually predominant [124]. In [124], the authors introduced a non-isolated dual-input–single-output DC-DC converter designed for both unidirectional and bidirectional power transfer applications involving PV and/or wind RES. The proposed topology addressed challenges related to discontinuous and pulsating input currents, ensuring a continuous input current. Additional topologies were investigated for their improved voltage gain and efficiency. Due to its larger switching duty cycle range, the multi-input–single-output DC-DC converter in [125] exhibited significant voltage gain, reduced current stress, and flexibility. Capacitor voltage accumulation allowed the double-input step-up converters based on switched-diode-capacitor voltage accumulation structures in [126] to achieve higher voltage gains. In [127], the authors proposed a high-step-up multiple-input boost converter, which provided significant step-up ratios for applications like PV grid-connected systems. The multiport Z-Quasi resonant DC-DC converter in [128] offered an improved step-up ratio and reduced switch voltage stress. For more effective power management, the dual-input–single-output converter in [129] featured six operation modes. The non-isolated three-port converter in [130] was integrated into PV, battery, and load ports, ensuring higher power density and reliability. The multi-input–single-output converter in [131] provided flexible control with increased voltage gain by adding more inputs and optimal voltage regulation. The non-isolated multi-input high-step-up DC-DC converter in [132] achieved a higher efficiency with fewer components and lower costs. Additionally, the dual-input high-step-up DC-DC converter with a zero-voltage transition auxiliary circuit in [133] improved efficiency and reduced costs for PV power generation systems, due to its simple control strategy and reduced component count. Despite these advanced features, the proposed converter outperformed these designs by achieving the highest voltage gain, enabling efficient power conversion even at low duty cycles, and achieving a maximum experimental efficiency of 94%, correlating with an output power of around 86 W.

In [134], the authors suggested a double-input–single-output pulse-width modulation (PWM) for high- and low-voltage sources, which was later used in [135] for modeling a small hybrid PV–wind DC water pumping system designed for remote regions in the Amazon. The suggested structure comprised buck and buck–boost converters with a common inductor and capacitor as filters. Though it is simple and able to operate in both step-down and step-up/down modes, the converter suffered from increased ripple and discontinuity in the input source current, output voltage drops, and reduced power delivery to the load due to the inability to transfer energy from input sources to the load and inductor simultaneously.

In [136], the authors proposed the doubler boost converter and the single-switch converter combined with voltage multiplier cells to address challenges related to limited voltage gain, which is insufficient for RE applications. Both topologies had one switch and inductor, aiming to reduce design complexity and cost. In the case of the doubler boost converter with a 12 V DC input operating at a duty ratio of 0.5 and a switching frequency of 40 kHz, the use of 10 voltage multiplier cells in cascade yielded up to 960 V of voltage rise. As for the switch boost converter using a 12 V DC input and operating at a duty ratio of 0.25 with a switching frequency of 5 kHz, cascading 10 voltage multiplier cells yielded up to 480 V of voltage increase.

In [137], the authors introduced a non-isolated high-gain three-port inverter featuring soft switching to tackle issues associated with incorporating a low-output-voltage RES and ESS into high-voltage DC buses. These challenges include diminished efficiency from numerous conversion stages, increased system cost due to a greater demand for active switches, and the necessity for complex control systems [75,138]. A laboratory prototype was designed using a 30 V RES and a 48 V ESS to verify its performance. The proposed converter achieved a high voltage gain, resulting in a 400 V output voltage and a maximum efficiency of 96% under a 180 W load while maintaining low voltage stress on the switches and reducing switch losses. However, it encountered challenges associated with discontinuous current flows, impacting RES performance and battery efficiency.

Table 4 summarizes the aforementioned hybrid converter topologies, along with their specific characteristics.

Table 4. Non-isolated converters for hybrid applications.

Topology	Name	Voltage Gain	Efficiency	Applications	Advantages	Disadvantages	Experimental Prototype
[124]	Dual input–single output	$\frac{3-D}{1-D^2}$	95%	Hybrid (PV and WT), stand-alone systems, including battery ESS and DC motor	• Bidirectional capability. • Continuous input current.	Complex control mechanisms.	150 W 10 V DC input 1 10 V DC input 2 100 V DC output
[125]	Multi-input–single output DC-DC converter	$\frac{D_2}{(1-D_1)(1-D_2)}$	98%	DC microgrid, grid-tied PV systems	• Ensures continuous input current. • Exhibits the highest voltage gain compared to [57–65], enabling efficient power conversion even at low duty cycles.	• The prototype experienced voltage variations and current fluctuations. • The performance is inconsistent.	86 W 20 V DC input 1 30 V DC input 2 95 V DC output
[136]	Doubler boost converter and the single-switch converter combined with voltage multiplier cells	$\frac{2N}{1-2D}$	-	PV and WT	• Simple structure. • Able to operate as buck and boost.	• Increased current ripples. • Discontinuous input source. • Output voltage drops. • Reduced power delivery to the load.	12 V DC input 480 V–960 V DC output
[137]	High-gain three-port inverter featuring soft switching	$\frac{N+2}{1-D}$	96%	PV and ESS	• Less complex control system, so lower cost. • High voltage gain. • Maintained low voltage stress on the switches. • Reduced switch losses.	Discontinuous current flows impacting performance of RES and battery efficiency.	180 W 30 V RES + 48 V ESS

4. Converter Topologies for AC-Powered HPs

4.1. AC-DC Topologies on WT Side

In the system shown in Figure 1, the WT interfaces with the DC-bus. Rectifiers play a crucial role in WT conversion chains, converting the AC power generated by the WT into DC power that can be utilized by the inverter. In a grid-connected system, a bidirectional AC-DC converter is employed between the AC grid and the DC-bus [139], allowing excess generated power to be exported to the AC grid or used to charge batteries via the DC-bus. Different rectifier technologies (shown in Figure 6) are used in WT systems, each offering various advantages and disadvantages in terms of control, performance, and cost. As illustrated in Figure 7, the conversion can occur in either one stage or two stages. A significant advantage of two-stage conversion is the voltage gain at the input of the DC-bus.

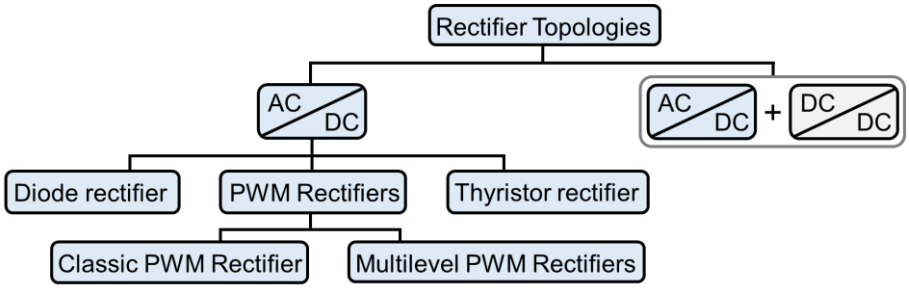

Figure 6. AC-DC rectifier classification.

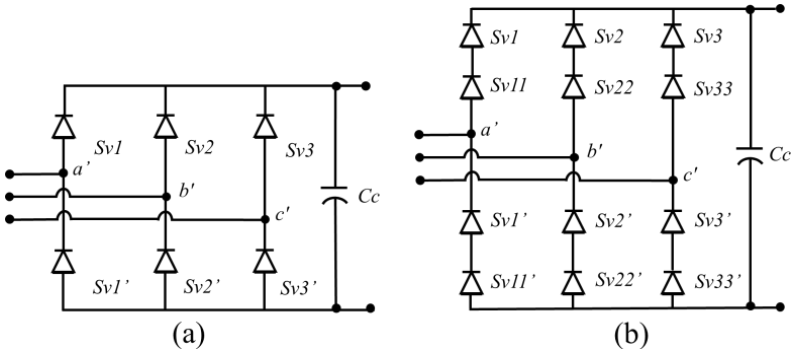

Figure 7. Diode rectifier used in (**a**) low-voltage and (**b**) medium-voltage applications, respectively.

AC-DC rectifiers are either controlled (thyristor, IGBT, MOSFET) or uncontrolled (diode) [140]. Diode rectifiers are the simplest and most cost-effective solution. However, they do not allow for control of the DC output voltage, which can be problematic in variable-speed WTs where the generator's voltage and frequency vary significantly. The classic topology shown in Figure 7a, typically dedicated to low-voltage applications, can be integrated into a medium-voltage power chain by adding diodes, as shown in Figure 7b [141].

One of their major drawbacks is the poor power factor and harmonics penetration on the AC side [142]. To overcome this, PWM rectifiers were introduced. PWM rectifiers offer better controllability and facilitate the optimization of the WT's operating point. These advantages make the PWM rectifier the preferred choice when integrating a controlled rectifier into a wind power conversion system. In some cases where the DC-bus requires higher voltage levels, a DC-DC high-step-up converter could be integrated with the AC-DC rectifier to boost the lower DC voltage from the rectifier to a higher DC voltage level.

Fully controlled rectifiers, also known as PWM rectifiers, are similar to those found in DC-AC conversion systems, with the primary difference lying in the control stage. Thus, the classic PWM rectifier is essentially a two-level voltage source converter (2L-VSC). This equivalence extends to multilevel topologies such as neutral point clamped (NPC), active

neutral point clamped (ANPC), and flying capacitor (FC), among which the NPC topology is the one broadly employed [143]. In fact, the 2L-VSC is utilized in 90% of WT applications with power ratings below 0.75 MW [144]. Converters used to integrate with a WT are compared primarily according to cost [145,146] (including maintenance), efficiency [147], output power quality, and the output voltage (sinusoidal shape with low total harmonic distortion) [148].

Table 5 examines the fundamental topologies of AC-DC converters, highlighting their merits and demerits. The basic topologies, both classic and multilevel, are illustrated in Figure 8.

Table 5. AC-DC topologies for WT side [143,144,149].

	2L-VSC	**3L-NPC**	**3L-ANPC**	**3L-FC**
Number of switches	12	24	36	24
Number of diodes	0	12	0	0
Number of capacitors	0	0	0	6
Device voltage stress	V_{dc}	$\frac{V_{dc}}{2}$	$\frac{V_{dc}}{2}$	$\frac{V_{dc}}{2}$
Power density	Moderate	High	High	High
Modularity	Low	Low	Low	High
Control complexity	Moderate	Medium	Medium	High
Harmonic performance	High	Low	Low	Low
Power	Limited 0.75 MW	High 3.0–12.0 MW	High 3.0–12.0 MW	High 3.0–12.0 MW

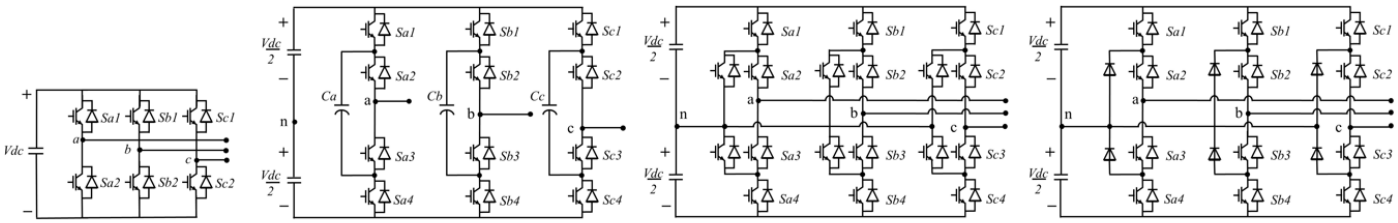

Figure 8. (**a**) 2L-VSC, (**b**) 3L-FC, (**c**) 3L-ANPC, and (**d**) 3L-NPC.

4.2. DC-AC Topologies on AC-Powered HP Side

Inverters are classified as either voltage-source or current-source converters. Voltage-source inverters are the second most common power converters [150]. They are also classified according to the AC output waveform (single-phase, used for residential applications, or three-phase, used for industrial applications). Voltage-source inverters are either classified as two-level or MLIs.

MLIs were introduced as emerging solutions to integrate with RES, such as PVs and WTs [151], to generate a multiple-step output voltage waveform, which decreases the voltage stress on power semiconductors. Table 6 briefly presents the advantages and disadvantages of MLIs. NPC and cascaded-H-bridge (CHB) are among the well-known MLI topologies. Their advantages and disadvantages are presented in Table 7.

Table 6. Advantages and disadvantages of MLIs [78,152].

Advantages	Disadvantages
• Reduced harmonic distortion • Generation of higher voltage levels, thus suitable for high-voltage and high-power applications • Staircase waveform quality • Operates at both fundamental and high-switching-frequency PWM • Lower switching losses • Better electromagnetic compatibility • Higher power quality	• Higher overall system cost and complexity due to the need for a large number of power semiconductor switches and gate driver circuit associated with each switch • Challenges in voltage balancing and capacitor management, leading to higher costs and maintenance requirements

CHB converters offer several key advantages. Their modularity and simple construction make it easy to adapt to high power and voltage levels. Additionally, the reduction of dv/dt minimizes stress on passive components and improves source current quality by reducing total harmonic distortion. Their reliability is also enhanced by the integration of inactive redundant modules and fault-tolerant control schemes, ensuring stable operation even with a large number of active devices. Furthermore, with appropriate control [153], they are favorable for fault detection and localization, making CHB converters an interesting topology for controlling HPs. However, while the CHB topology addresses some drawbacks of the NPC and FC topologies—such as the need for clamp diodes and additional capacitors—its modularity, which is advantageous for certain applications, can be a drawback in others, particularly in an energy mix. Specifically, its connection to a common DC-bus, as in the system described in Figure 1, can become quite complex. Therefore, this topology might not be optimal in such configurations.

Table 7. Comparison of the basic MLI topologies.

MLI Topology	Advantages	Disadvantages
NPC [154–156]	Can be extended to higher power rates and more output voltage levels by adding additional power switches and clamping diodes (up to three levels only)	Technical challenges in high-power applications such as voltage unbalances and reverse recovery stress.
CHB [116]	For the same number of levels, cascaded-H-bridge converters are highly modular and reliable, requiring fewer components	Each module requires different sources of DC voltage or capacitors. The large number of capacitors necessitates a more complex controller.
FC [156,157]	• Can be more easily extended to achieve more voltage levels and higher power rates, due to its modular structure • Good voltage balancing	Higher number of capacitors.

Hybrid topologies are a branch of MLIs that has gained more attention in the literature as they create an efficient system that integrates the advantages of both types of converters. In [158], the authors proposed a switched-capacitor single-source cascaded MLI that uses only one DC source, with the remaining DC sources replaced by capacitors, making it suitable for grid-tied PV systems by eliminating leakage current and boosting input voltage. In addition, a charging inductor, connected to a freewheeling diode, is integrated in series with the DC source to reduce inrush currents. Although the topology proposed in [151] offers several advantages, such as eliminating the need for a boost circuit by

relying on a single-input voltage source and eliminating leakage current, it might require complex control strategies for practical applications to ensure consistent and reliable voltage balancing across all capacitors. Furthermore, the number of switches is high, which leads to a higher cost. This issue is resolved in [159], where only six power switches, two switched capacitors, and one power diode were used for five-level operation. Additionally, the capacitors are naturally balanced, eliminating the need for additional control methods or sensors.

Table 8 summarizes the aforementioned DC-AC isolated converter topologies, along with their specific characteristics.

Table 8. DC-AC isolated converters for AC-powered HPs.

Topology	Name	Efficiency	Advantages	Disadvantages	Experimental Prototype
[151]	Modified switched-capacitor MLI	96%	• Eliminates leakage current. • Eliminates the need for a boost circuit by relying on a single-input voltage source.	• Requires complex control strategies for practical applications to ensure consistent and reliable voltage balancing across all capacitors. • Expensive because the number of switches is high.	500 W 183 V DC input 220 V AC output
[158]	Switched-capacitor single-source cascaded MLI	-	• Eliminates leakage current. • Reduces inrush currents. • Boosts input voltage.	• Suffers from discontinuous input current. • Loses common ground feature.	275 W 80 V DC input 311 V AC output
[159]	Five-level transformer-less inverter with self-voltage balancing and boosting ability	98%	• Less expensive. • Eliminates the need for additional control methods and sensors because the capacitors are naturally balanced.	Requires complex control strategies.	1 kW 100 V DC input 200 V AC output

The crucial interplay between energy management strategies and control methods plays a significant role in the context of converter topologies. Modulation strategies, which generate signals to control the operation of power switches, guide the converter's circuit principle. These control signals are derived from control algorithms [160] that monitor the system's voltage and/or current to the desired levels and adjust them accordingly. It is important to emphasize that the power stage can only meet the load's requirements with an appropriate control method. Various modulation strategies can be employed to control a static converter, including PWM, step or staircase control, angle variation control (specific to thyristor control), and hysteresis control [161,162].

PWM is the most widely used control method in power electronics [163–166]. This modulation strategy is specific to VSCs and can be applied to various types of conversions. It has also seen significant development in AC conversion [167], with its two main categories being scalar PWM and vector PWM. These two categories have been further extended to multilevel conversion, as shown in Figure 9.

- Scalar or sinusoidal PWM [168]: It compares the carrier signal to the reference signal. If the reference signal is higher, the output voltage is set to its maximum. Otherwise, the output voltage is set to its minimum. Thus, it generates a modulated voltage. This control strategy can be used with all types of converters (rectifiers, inverters, and choppers). In contrast, vector PWM is specifically applicable only to DC-AC and AC-DC converters. In addition to conventional PWM techniques, a digital logic-based

dead zone compensation method was proposed in [169] to improve the performance of H-bridge converters. This method adjusts the PWM signals based on the current polarity to mitigate total harmonic distortions caused by dead zones, enhancing AC output quality and ensuring compatibility with various control and modulation strategies. Its independence from specific control strategies enables straightforward adaptation to other converter types, such as NPC converters.

- Vector PWM [170]: This method involves using a vector-based approach to control the output. Instead of comparing signals directly, it transforms the reference signal into a two-dimensional vector using a mathematical transformation (like Park's transformation). The PWM process then modulates the output based on this vector representation. This allows for more precise control of the output voltage in systems with multiple phases or complex waveforms.

While Figure 9 presents the so-called conventional strategies, other approaches exist, such as the single-carrier strategy [171], which reduces the number of carriers and therefore decreases the computation time, discontinuous control methods that can impact power losses and improve efficiency [160], and voltage-balancing techniques [172].

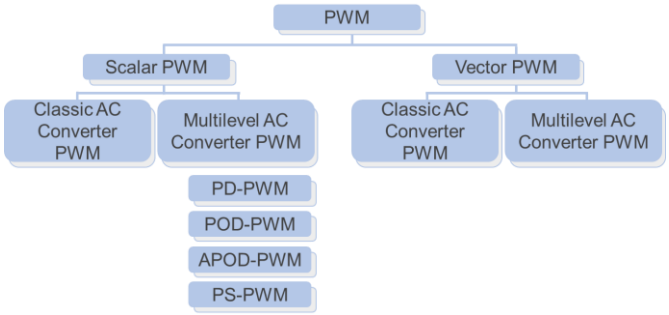

Figure 9. Classification of PWM techniques.

As mentioned earlier, the modulation strategies are implemented based on the signals generated by the control stage. This stage can be configured using different methods, depending on the specifications:

- Proportional-integral, proportional-derivative, or proportional-integral-derivative control: These controllers are commonly used in systems where stability is crucial, because of their simplicity and effectiveness, particularly in steady-state conditions [173].
- MPC: This architecture is based on a dynamic model of the system to predict its future behavior and optimize control actions. It is used in complex systems where constraints need to be managed [174,175].
- H-Infinity control: This approach is powerful for designing robust controllers capable of maintaining acceptable performance in uncertain environments. It is particularly suited for systems where reliability and robustness are essential [176].
- Fuzzy control: This method uses fuzzy logic to manage uncertainty and imprecision in control systems. It stands out in applications where mathematical models are difficult to establish [177].
- Sliding mode control: This is a robust controller that keeps the system state on a sliding surface. It is applied in nonlinear systems and those subject to uncertainties [178,179].

5. Conclusions and Future Research

HPs have clearly demonstrated their potential as a sustainable and versatile solution for heating and cooling applications. Their ability to be powered by RES makes them a key tool in achieving sustainable development goals. This comprehensive review of power converter topologies that could potentially be integrated with HPs highlights both the advances made in this field and the existing gaps and challenges. It is now crucial to continue research to further optimize these converter technologies for seamless and

efficient integration of HPs into RE systems. Future research directions should focus on developing new converter topologies that are more efficient, reliable, and cost effective. Special attention should also be given to improving compatibility between HPs and various RES to fully leverage their synergies. Additionally, exploring different modulation and control strategies capable of operating HPs under optimal conditions should be prioritized. In summary, this work provides a foundation for researchers and industry stakeholders aiming to advance converter technologies in the HP sector, contributing to a more sustainable energy transition.

Author Contributions: Methodology, J.A. and M.B.C.; formal analysis, J.A.; writing—original draft preparation, J.A. and J.S.M.; writing—review and editing, J.A., M.B.C., D.G. and B.D.; supervision, M.B.C. and D.G.; project administration, M.B.C. All authors have read and agreed to the published version of the manuscript.

Funding: This work was performed within the framework of the Interreg Waterwarmth project, co-funded by the European Union and University of Le Havre Normandie.

Data Availability Statement: Data are contained within the article.

Acknowledgments: This work was performed at the GREAH Laboratory, University of Le Havre Normandie, particularly by the research team of Renewable Energies and Storage Systems (MERS). The authors would like to thank the European Union and University of Le Havre Normandie for their financial support.

Conflicts of Interest: The authors declare no conflicts of interest.

Abbreviations

AC	Alternating Current
ASHP	Air-Source Heat Pump
ANPC	Active Neutral Point Clamped
BDC	Bidirectional Converter
CHB	Cascaded H-Bridge
DAB	Dual Active Bridge
DC	Direct Current
DHB	Dual Half-Bridge
ESS	Energy Storage Systems
FC	Flying Capacitor
GSHP	Ground-Source Heat Pump
HP	Heat Pump
MLI	Multilevel Inverter
MPC	Model Predictive Control
NPC	Neutral Point Clamped
PV	Photovoltaic
PWM	Pulse-Width Modulation
RC	Resonant Converter
RE	Renewable Energy
RES	Renewable Energy Sources
VMC	Voltage Multiplier Cell
VSC	Voltage-Source Converter
WSHP	Water-Source Heat Pump
WT	Wind Turbine
ZCS	Zero Current Switching
ZVS	Zero Voltage Switching

References

1. Eurostat Heating and Cooling from Renewables Gradually Increasing—Products Eurostat News—Eurostat. Available online: https://ec.europa.eu/eurostat/en/web/products-eurostat-news/w/ddn-20230203-1 (accessed on 19 February 2024).

2. International Energy Agency (IEA). Tracking Heating. Available online: https://www.iea.org/energy-system/buildings/heating#tracking (accessed on 27 February 2024).
3. Energy Education Heat Pump. Available online: https://energyeducation.ca/encyclopedia/Heat_pump#:~:text=The%20heating%20cycle%20of%20a,air,%20turning%20into%20a%20gas (accessed on 24 January 2024).
4. Sadeghi, H.; Ijaz, A.; Singh, R.M. Current Status of Heat Pumps in Norway and Analysis of Their Performance and Payback Time. *Sustain. Energy Technol. Assess.* **2022**, *54*, 102829. [CrossRef]
5. Gilani, H.A.; Hoseinzadeh, S.; Karimi, H.; Karimi, A.; Hassanzadeh, A.; Garcia, D.A. Performance Analysis of Integrated Solar Heat Pump VRF System for the Low Energy Building in Mediterranean Island. *Renew. Energy* **2021**, *174*, 1006–1019. [CrossRef]
6. Bloess, A.; Schill, W.P.; Zerrahn, A. Power-to-Heat for Renewable Energy Integration: A Review of Technologies, Modeling Approaches, and Flexibility Potentials. *Appl. Energy* **2018**, *212*, 1611–1626. [CrossRef]
7. Peskova, M. Data-Driven Models for Estimating Heat Pump Power. Master's Thesis, Department of Energy Technology, KTH Royal Institute of Technology, Industrial Engineering and Management, Stockholm, Sweden, 2023.
8. Lorenzo, C.; Narvarte, L.; Almeida, R.H.; Cristóbal, A.B. Technical Evaluation of a Stand-Alone Photovoltaic Heat Pump System without Batteries for Cooling Applications. *Sol. Energy* **2020**, *206*, 92–105. [CrossRef]
9. Fischer, D.; Madani, H. On Heat Pumps in Smart Grids: A Review. *Renew. Sustain. Energy Rev.* **2017**, *70*, 342–357. [CrossRef]
10. Baraskar, S.; Günther, D.; Wapler, J.; Lämmle, M. Analysis of the Performance and Operation of a Photovoltaic-Battery Heat Pump System Based on Field Measurement Data. *Sol. Energy Adv.* **2023**, *4*, 100047. [CrossRef]
11. Lawan, M.M.G.; Raharijaona, J.; Camara, M.B.; Dakyo, B. Power Control for Decentralized Energy Production System Based on the Renewable Energies—Using Battery to Compensate the Wind/Load/PV Power Fluctuations. In Proceedings of the 2017 IEEE 6th International Conference on Renewable Energy Research and Applications (ICRERA), San Diego, CA, USA, 5–8 November 2017; pp. 1132–1138. [CrossRef]
12. Boroyevich, D.; Cvetkovic, I.; Burgos, R.; Dong, D. Intergrid: A Future Electronic Energy Network? *IEEE J. Emerg. Sel. Top. Power Electron.* **2013**, *1*, 127–138. [CrossRef]
13. Zhang, G.; Li, Z.; Zhang, B.; Halang, W.A. Power Electronics Converters: Past, Present and Future. *Renew. Sustain. Energy Rev.* **2018**, *81*, 2028–2044. [CrossRef]
14. Justo, J.J.; Mwasilu, F.; Lee, J.; Jung, J.W. AC-Microgrids versus DC-Microgrids with Distributed Energy Resources: A Review. *Renew. Sustain. Energy Rev.* **2013**, *24*, 387–405. [CrossRef]
15. Henning, H.M.; Palzer, A. A Comprehensive Model for the German Electricity and Heat Sector in a Future Energy System with a Dominant Contribution from Renewable Energy Technologies—Part I: Methodology. *Renew. Sustain. Energy Rev.* **2014**, *30*, 1003–1018. [CrossRef]
16. Hannan, M.A.; Lipu, M.S.H.; Ker, P.J.; Begum, R.A.; Agelidis, V.G.; Blaabjerg, F. Power Electronics Contribution to Renewable Energy Conversion Addressing Emission Reduction: Applications, Issues, and Recommendations. *Appl. Energy* **2019**, *251*, 113404. [CrossRef]
17. Zhang, N.; Sutanto, D.; Muttaqi, K.M. A Review of Topologies of Three-Port DC-DC Converters for the Integration of Renewable Energy and Energy Storage System. *Renew. Sustain. Energy Rev.* **2016**, *56*, 388–401. [CrossRef]
18. Hossain, M.Z.; Rahim, N.A.; Selvaraj, J.a/l. Recent Progress and Development on Power DC-DC Converter Topology, Control, Design and Applications: A Review. *Renew. Sustain. Energy Rev.* **2018**, *81*, 205–230. [CrossRef]
19. Roy, P.; He, J.; Zhao, T.; Singh, Y.V. Recent Advances of Wind-Solar Hybrid Renewable Energy Systems for Power Generation: A Review. *IEEE Open J. Ind. Electron. Soc.* **2022**, *3*, 81–104. [CrossRef]
20. Toure, M.L.; Camara, M.B.; Payman, A.; Dakyo, B. African Renewable Energy Potentialities Review for Local Weak Grids Reinforcement Study. In Proceedings of the 2023 11th International Conference on Smart Grid (icSmartGrid), Paris, France, 4–7 June 2023; pp. 388–397. [CrossRef]
21. Poulet, P.; Outbib, R. Energy Production for Dwellings by Using Hybrid Systems Based on Heat Pump Variable Input Power. *Appl. Energy* **2015**, *147*, 413–429. [CrossRef]
22. Fischer, D.; Rautenberg, F.; Wirtz, T.; Wille-Haussmann, B.; Madani, H. Smart Meter Enabled Control for Variable Speed Heat Pumps to Increase PV Self-Consumption. *Refrig. Sci. Technol.* **2015**, *24*, 4049–4056. [CrossRef]
23. Laine, H.S.; Salpakari, J.; Looney, E.E.; Savin, H.; Peters, I.M.; Buonassisi, T. Meeting Global Cooling Demand with Photovoltaics during the 21st Century. *Energy Environ. Sci.* **2019**, *12*, 2706–2716. [CrossRef]
24. Rieck, J.; Taube, L.; Behrendt, F. Feasibility Analysis of a Heat Pump Powered by Wind Turbines and PV- Applications for Detached Houses in Germany. *Renew. Energy* **2020**, *162*, 1104–1112. [CrossRef]
25. Bojić, M.; Nikolić, N.; Nikolić, D.; Skerlić, J.; Miletić, I. Toward a Positive-Net-Energy Residential Building in Serbian Conditions. *Appl. Energy* **2011**, *88*, 2407–2419. [CrossRef]
26. Roselli, C.; Sasso, M.; Tariello, F. Dynamic Simulation of a Solar Electric Driven Heat Pump for an Office Building Located in Southern Italy. *Int. J. Heat Technol.* **2016**, *34*, S496–S504. [CrossRef]
27. Klokov, A.V.; Tutunin, A.S.; Sharaborova, E.S.; Korshunov, A.A.; Loktionov, E.Y. Inverter Heat Pumps as a Variable Load for Off-Grid Solar-Powered Systems. *Energies* **2023**, *16*, 5987. [CrossRef]
28. Izquierdo, M.; De Agustín, P.; Martín, E. A Micro Photovoltaic-Heat Pump System for House Heating by Radiant Floor: Some Experimental Results. *Energy Procedia* **2014**, *48*, 865–875. [CrossRef]

29. Franco, A.; Fantozzi, F. Experimental Analysis of a Self-Consumption Strategy for Residential Building: The Integration of PV System and Geothermal Heat Pump. *Renew. Energy* **2016**, *86*, 1075–1085. [CrossRef]
30. Aguilar, F.; Crespí-Llorens, D.; Quiles, P.V. Techno-Economic Analysis of an Air Conditioning Heat Pump Powered by Photovoltaic Panels and the Grid. *Sol. Energy* **2019**, *180*, 169–179. [CrossRef]
31. Aguilar, F.J.; Aledo, S.; Quiles, P.V. Experimental Analysis of an Air Conditioner Powered by Photovoltaic Energy and Supported by the Grid. *Appl. Therm. Eng.* **2017**, *123*, 486–497. [CrossRef]
32. Charalambous, C.; Heracleous, C.; Michael, A.; Efthymiou, V. Hybrid AC-DC Distribution System for Building Integrated Photovoltaics and Energy Storage Solutions for Heating-Cooling Purposes. A Case Study of a Historic Building in Cyprus. *Renew. Energy* **2023**, *216*, 119032. [CrossRef]
33. Fapi, C.B.N.; Touré, M.L.; Camara, M.-B.; Dakyo, B. High Voltage Gain DC-DC Converter Based Maximum Power Tracking from Photovoltaic Systems for Heat-Pump Applications. In Proceedings of the 2024 12th International Conference on Smart Grid (icSmartGrid), Shanghai, China, 25–27 October 2024; pp. 493–498.
34. Han, S.; Li, X.; Zhao, W.; Wang, L.; Liang, A.; Zeng, S. Simulation Study of the Control Strategy of a DC Inverter Heat Pump Using a DC Distribution Network. *Energy Eng. J. Assoc. Energy Eng.* **2023**, *120*, 1421–1444. [CrossRef]
35. Ekren, O.; Celik, S.; Noble, B.; Krauss, R. Performance Evaluation of a Variable Speed DC Compressor. *Int. J. Refrig.* **2013**, *36*, 745–757. [CrossRef]
36. Vossos, V.; Garbesi, K.; Shen, H. Energy Savings from Direct-DC in U.S. Residential Buildings. *Energy Build.* **2014**, *68*, 223–231. [CrossRef]
37. Zaid, M.; Malick, I.H.; Ashraf, I.; Tariq, M.; Alamri, B.; Rodrigues, E.M.G. A Non-isolated Transformerless High-Gain DC–DC Converter for Renewable Energy Applications. *Electronics* **2022**, *11*, 2014. [CrossRef]
38. Changchien, S.K.; Liang, T.J.; Chen, J.F.; Yang, L.S. Novel High Step-up DCDC Converter for Fuel Cell Energy Conversion System. *IEEE Trans. Ind. Electron.* **2010**, *57*, 2007–2017. [CrossRef]
39. Forouzesh, M.; Siwakoti, Y.P.; Gorji, S.A.; Blaabjerg, F.; Lehman, B. Step-Up DC-DC Converters: A Comprehensive Review of Voltage-Boosting Techniques, Topologies, and Applications. *IEEE Trans. Power Electron.* **2017**, *32*, 9143–9178. [CrossRef]
40. Tomaszuk, A.; Krupa, A. High Efficiency High Step-up DC/DC Converters—A Review. *Bull. Pol. Acad. Sci. Tech. Sci.* **2011**, *59*, 475–483. [CrossRef]
41. Saravanan, S.; Ramesh Babu, N. Analysis and Implementation of High Step-up DC-DC Converter for PV Based Grid Application. *Appl. Energy* **2017**, *190*, 64–72. [CrossRef]
42. Samiullah, M.; Siddique, M.D.; Iqbal, A.; Maroti, P.K.; Banerjee, S. A Non-Isolated Symmetrical Design of Voltage Lift Switched-Inductor Boost Converter with Higher Gain and Low Voltage Stress across Switches. *IET Power Electron.* **2022**. [CrossRef]
43. Ahmed, H.Y.; Abdel-rahim, O.; Ali, Z.M. New High Gain Transformerless DC/DC Boost System. *Electronics* **2022**, *11*, 734. [CrossRef]
44. Matsui, K.; Yamamoto, I.; Kishi, T.; Hasegawa, M.; Mori, H.; Ueda, F. A Comparison of Various Buck-Boost Converters and Their Application to PFC. *IECON Proc. (Ind. Electron. Conf.)* **2002**, *1*, 30–36. [CrossRef]
45. Marjani, J.; Imani, A.; Hekmati, A.; Afjei, E. A New Dual Output DC-DC Converter Based on SEPIC and Cuk Converters. In Proceedings of the 2016 International Symposium on Power Electronics, Electrical Drives, Automation and Motion (SPEEDAM), Capri, Italy, 22–24 June 2016; pp. 946–950. [CrossRef]
46. Banaei, M.R.; Bonab, H.A.F. A High Efficiency Non-isolated Buck-Boost Converter Based on ZETA Converter. *IEEE Trans. Ind. Electron.* **2020**, *67*, 1991–1998. [CrossRef]
47. Newlin, D.J.S.; Ramalakshmi, R.; Rajasekaran, S. A Performance Comparison of Interleaved Boost Converter and Conventional Boost Converter for Renewable Energy Application. In Proceedings of the 2013 International Conference on Green High-Performance Computing (ICGHPC), Nagercoil, India, 14–15 March 2013. [CrossRef]
48. Soltani, M.; Mostaan, A.; Siwakoti, Y.P.; Davari, P.; Blaabjerg, F. Family of Step-up DC/DC Converters with Fast Dynamic Response for Low Power Applications. *IET Power Electron.* **2016**, *9*, 2665–2673. [CrossRef]
49. Zhao, Q.; Tao, F.; Lee, F.C.; Xu, P.; Wei, J. A Simple and Effective Method to Alleviate the Rectifier Reverse-Recovery Problem in Continuous-Current-Mode Boost Converters. *IEEE Trans. Power Electron.* **2001**, *16*, 649–658. [CrossRef]
50. Chen, J.; Maksimović, D.; Erickson, R.W. Analysis and Design of a Low-Stress Buck-Boost Converter in Universal-Input PFC Applications. *IEEE Trans. Power Electron.* **2006**, *21*, 320–329. [CrossRef]
51. Abusorrah, A.; Al-Hindawi, M.M.; Al-Turki, Y.; Mandal, K.; Giaouris, D.; Banerjee, S.; Voutetakis, S.; Papadopoulou, S. Stability of a Boost Converter Fed from Photovoltaic Source. *Sol. Energy* **2013**, *98*, 458–471. [CrossRef]
52. dos Reis Barbosa, L.; Sousa Vilefort, L.; Vincenzi Romualdo da Silva, F.; Antônio Alves Coelho, E.; Carlos Gomes de Freitas, L.; Carlos de Freitas, L.; Batista Vieira Júnior, J. Analysis of A Soft-Single-Switched Quadratic Boost Converter. *Eletrônica De Potência* **2013**, *18*, 1047–1054. [CrossRef]
53. Meshael, H.; Elkhateb, A.; Best, R. Topologies and Design Characteristics of Isolated High Step-Up DC–DC Converters for Photovoltaic Systems. *Electronics* **2023**, *12*, 3913. [CrossRef]
54. Ren, B.; Wang, D.; Mao, C.; Qiu, J.; Zhao, J. Analysis of Full Bridge DC-DC Converter in Power System. In Proceedings of the 2011 4th International Conference on Electric Utility Deregulation and Restructuring and Power Technologies (DRPT), Weihai, China, 6–9 July 2011; pp. 1242–1245. [CrossRef]

55. Farajdadian, S.; Hajizadeh, A.; Soltani, M. Recent Developments of Multiport DC/DC Converter Topologies, Control Strategies, and Applications: A Comparative Review and Analysis. *Energy Rep.* **2024**, *11*, 1019–1052. [CrossRef]
56. Hashemzadeh, S.M.; Hosseini, S.H.; Babaei, E.; Sabahi, M. Design and Modelling of a New Three Winding Coupled Inductor Based High Step-up DC–DC Converter for Renewable Energy Applications. *IET Power Electron.* **2022**, *15*, 1322–1339. [CrossRef]
57. Talebi, P.; Packnezhad, M.; Farzanehfard, H. Single-Switch High Step-Up Y-Source-Boost Converter for Renewable Energy Applications. *IEEE Trans. Ind. Electron.* **2024**, *71*, 1–8. [CrossRef]
58. Siwakoti, Y.P.; Loh, P.C.; Blaabjerg, F.; Andreasen, S.J.; Town, G.E. Y-Source Boost DC/DC Converter for Distributed Generation. *IEEE Trans. Ind. Electron.* **2015**, *62*, 1059–1069. [CrossRef]
59. Ji, Y.; Liu, H.; Feng, Y.; Wu, F.; Wheeler, P. High Step-Up Y-Source Coupled-Inductor Impedance Network Boost DC-DC Converters with Common Ground and Continuous Input Current. *IEEE J. Emerg. Sel. Top. Power Electron.* **2020**, *8*, 3174–3183. [CrossRef]
60. Lee, S.W.; Do, H.L. Quadratic Boost DC-DC Converter with High Voltage Gain and Reduced Voltage Stresses. *IEEE Trans. Power Electron.* **2019**, *34*, 2397–2404. [CrossRef]
61. Jalilzadeh, T.; Rostami, N.; Babaei, E.; Maalandish, M. Non-isolated Topology for High Step-Up DC-DC Converters. *IEEE J. Emerg. Sel. Top. Power Electron.* **2023**, *11*, 1154–1168. [CrossRef]
62. Forouzesh, M.; Shen, Y.; Yari, K.; Siwakoti, Y.P.; Blaabjerg, F. High-Efficiency High Step-Up DC-DC Converter with Dual Coupled Inductors for Grid-Connected Photovoltaic Systems. *IEEE Trans. Power Electron.* **2018**, *33*, 5967–5982. [CrossRef]
63. Hashemzadeh, S.M.; Hosseini, S.H.; Babaei, E.; Sabahi, M. A Soft Switched High Step-up DC-DC Converter Based on VMC and Coupled Inductor for Photovoltaic Energy Applications. *IET Renew. Power Gener.* **2023**, *17*, 1583–1596. [CrossRef]
64. Rao, C.; Hajjiah, A.; El-Meligy, M.A.; Sharaf, M.; Soliman, A.T.; Mohamed, M.A. A Novel High-Gain Soft-Switching DC-DC Converter with Improved PO MPPT for Photovoltaic Applications. *IEEE Access* **2021**, *9*, 58790–58806. [CrossRef]
65. Yao, Q.; Zeng, Y.; Jia, Q. A Novel Non-Isolated Cubic DC-DC Converter with High Voltage Gain for Renewable Energy Power Generation System. *Energy Eng. J. Assoc. Energy Eng.* **2024**, *121*, 221–241. [CrossRef]
66. Chen, W.; Wu, X.; Yao, L.; Jiang, W.; Hu, R. A Step-up Resonant Converter for Grid-Connected Renewable Energy Sources. *IEEE Trans. Power Electron.* **2015**, *30*, 3017–3029. [CrossRef]
67. Abdel-Rahim, O.; Wang, H. A New High Gain DC-DC Converter with Model-Predictive-Control Based MPPT Technique for Photovoltaic Systems. *CPSS Trans. Power Electron. Appl.* **2020**, *5*, 191–200. [CrossRef]
68. Subhani, N.; May, Z.; Alam, M.K.; Khan, I.; Hossain, M.A.; Mamun, S. An Improved Non-Isolated Quadratic DC-DC Boost Converter with Ultra High Gain Ability. *IEEE Access* **2023**, *11*, 11350–11363. [CrossRef]
69. Vakacharla, V.R.; Rathore, A.K. Isolated Soft Switching Current Fed LCC-T Resonant DC-DC Converter for PV/Fuel Cell Applications. *IEEE Trans. Ind. Electron.* **2019**, *66*, 6947–6958. [CrossRef]
70. Akhlaghi, Z.; Karimi, A.; Adib, E. High Step-up DC–DC Converter with Low Conduction Losses and Reduced Switching Losses. *IET Renew. Power Gener.* **2024**, *18*, 654–662. [CrossRef]
71. Lee, S.W.; Do, H.L. Isolated High Step-Up Dual-Flyback DC–DC Converter with a Resonant Voltage Multiplier. *Electr. Power Compon. Syst.* **2020**, *48*, 871–880. [CrossRef]
72. Hasan, R.; Hassan, W.; Xiao, W. A High Gain Flyback DC-DC Converter for PV Applications. In Proceedings of the 2020 IEEE Region 10 Conference (TENCON), Osaka, Japan, 16–19 November 2020; pp. 522–526. [CrossRef]
73. Konar, S.; Saha, S.S. Efficient Energy Recovery and Boosting the Voltage Gain of a Soft-Switched Flyback Converter. In Proceedings of the 2020 IEEE International Conference on Power Electronics, Drives and Energy Systems (PEDES), Jaipur, India, 16–19 December 2020; pp. 1–5. [CrossRef]
74. Jiao, Y.; Li, B.; Ding, L.; Suo, Z.; Xu, D. DC/DC Converter with High Current Capability for All DC Renewable System. *IEEE Trans. Power Electron.* **2024**, *39*, 1–5. [CrossRef]
75. Shang, M.; Wang, H.; Cao, Q. Reconfigurable LLC Topology with Squeezed Frequency Span for High-Voltage Bus-Based Photovoltaic Systems. *IEEE Trans. Power Electron.* **2018**, *33*, 3688–3692. [CrossRef]
76. Sovacool, B.K. The Intermittency of Wind, Solar, and Renewable Electricity Generators: Technical Barrier or Rhetorical Excuse? *Util. Policy* **2009**, *17*, 288–296. [CrossRef]
77. Farhadi, M.; Mohammed, O. Energy Storage Technologies for High-Power Applications. *IEEE Trans. Ind. Appl.* **2016**, *52*, 1953–1962. [CrossRef]
78. Alatai, S.; Salem, M.; Ishak, D.; Das, H.S.; Nazari, M.A.; Bughneda, A.; Kamarol, M. A Review on State-of-the-Art Power Converters: Bidirectional, Resonant, Multilevel Converters and Their Derivatives. *Appl. Sci.* **2021**, *11*, 10172. [CrossRef]
79. Reddy, B.M.; Samuel, P. Analysis of Secluded Bi-Direction DC/DC Converters for the Performance Enhancement of Photo-Voltaic System and Energy Storage System. In Proceedings of the 2016 IEEE 7th Power India International Conference (PIICON), Bikaner, India, 25–27 November 2016. [CrossRef]
80. Mohammadi, M.R.; Farzanehfard, H. A New Bidirectional ZVS-PWM Cuk Converter with Active Clamp. In Proceedings of the 2011 19th Iranian Conference on Electrical Engineering, Tehran, Iran, 17–19 May 2011.
81. Meher, J.; Gosh, A. Comparative Study of DC/DC Bidirectional SEPIC Converter with Different Controllers. In Proceedings of the 2018 IEEE 8th Power India International Conference (PIICON), Kurukshetra, India, 10–12 December 2018; pp. 1–6. [CrossRef]
82. Zhang, Y.; Gao, Y.; Zhou, L.; Sumner, M. A Switched-Capacitor Bidirectional DC-DC Converter with Wide Voltage Gain Range for Electric Vehicles with Hybrid Energy Sources. *IEEE Trans. Power Electron.* **2018**, *33*, 9459–9469. [CrossRef]

83. Wang, F.; Luo, Y.; Li, H.; Xu, X. Switching Characteristics Optimization of Two-Phase Interleaved Bidirectional DC/DC for Electric Vehicles. *Energies* **2019**, *12*, 378. [CrossRef]
84. He, P.; Khaligh, A. Comprehensive Analyses and Comparison of 1 KW Isolated DC-DC Converters for Bidirectional EV Charging Systems. *IEEE Trans. Transp. Electrif.* **2017**, *3*, 147–156. [CrossRef]
85. De Doncker, R.W.A.A.; Divan, D.M.; Kheraluwala, M.H. A Three-Phase Soft-Switched High-Power-Density DC/DC Converter for High-Power Applications. *IEEE Trans. Ind. Appl.* **1991**, *27*, 63–73. [CrossRef]
86. Higa, H.; Takuma, S.; Orikawa, K.; Itoh, J.I. Dual Active Bridge DC-DC Converter Using Both Full and Half Bridge Topologies to Achieve High Efficiency for Wide Load. In Proceedings of the 2015 IEEE Energy Conversion Congress and Exposition (ECCE), Montreal, QC, Canada, 20–24 September 2015; pp. 6344–6351. [CrossRef]
87. Babokany, A.S.; Jabbari, M.; Shahgholian, G.; Mahdavian, M. A Review of Bidirectional Dual Active Bridge Converter. In Proceedings of the 2012 9th International Conference on Electrical Engineering/Electronics, Computer, Telecommunications and Information Technology, Phetchaburi, Thailand, 16–18 May 2012; Volume 2, pp. 1–4. [CrossRef]
88. Chub, A.; Vinnikov, D.; Kosenko, R.; Liivik, E.; Galkin, I. Bidirectional DC-DC Converter for Modular Residential Battery Energy Storage Systems. *IEEE Trans. Ind. Electron.* **2020**, *67*, 1944–1955. [CrossRef]
89. Xiong, H.; Song, D.; Shi, F.; Wei, Y.; Jinzhen, L. Novel Voltage Equalization Circuit of the Lithium Battery Pack Based on Bidirectional Flyback Converter. *IET Power Electron.* **2020**, *13*, 2194–2200. [CrossRef]
90. Gorji, S.A.; Ektesabi, M.; Zheng, J. Isolated Switched-Boost Push-Pull DC-DC Converter for Step-up Applications. *Electron. Lett.* **2017**, *53*, 177–179. [CrossRef]
91. Monteiro, J.; Pires, V.F.; Foito, D.; Cordeiro, A.; Silva, J.F.; Pinto, S. A Buck-Boost Converter with Extended Duty-Cycle Range in the Buck Voltage Region for Renewable Energy Sources. *Electronics* **2023**, *12*, 584. [CrossRef]
92. Mukherjee, S.; Kumar, A.; Chakraborty, S. Comparison of DAB and LLC DC-DC Converters in High-Step-Down Fixed-Conversion-Ratio (DCX) Applications. *IEEE Trans. Power Electron.* **2021**, *36*, 4383–4398. [CrossRef]
93. Hui, S.Y.R.; Chung, H.S.H. Resonant and Soft-Switching Converters. In *Power Electronics Handbook*; Elsevier: Amsterdam, The Netherlands, 2011; pp. 409–453.
94. Dobi, A.H.M.; Sahid, M.R.; Sutikno, T. Overview of Soft-Switching DC-DC Converters. *Int. J. Power Electron. Drive Syst.* **2018**, *9*, 2006–2018. [CrossRef]
95. Arazi, M.; Payman, A.; Camara, M.B.; Dakyo, B. Study of Different Topologies of DC-DC Resonant Converters for Renewable Energy Applications. In Proceedings of the 2018 Thirteenth International Conference on Ecological Vehicles and Renewable Energies (EVER), Monte Carlo, Monaco, 10–12 April 2018; pp. 1–6. [CrossRef]
96. Moorthy, R.S.K.; Rathore, A.K. Zero Current Switching Current-Fed Parallel Resonant Push-Pull (CFPRPP) Converter. In Proceedings of the 2014 International Power Electronics Conference (IPEC-Hiroshima 2014-ECCE ASIA), Hiroshima, Japan, 18–21 May 2014; pp. 3616–3623.
97. Alam, M.A.; Minai, A.F.; Bakhsh, F.I. Isolated Bidirectional DC-DC Converter: A Topological Review. *e-Prime-Adv. Electr. Eng. Electron. Energy* **2024**, *8*, 100594. [CrossRef]
98. Mudiyanselage, G.A.; Keshmiri, N.; Emadi, A. A Review of DC-DC Resonant Converter Topologies and Control Techniques for Electric Vehicle Applications. *IEEE Open J. Power Electron.* **2023**, *4*, 945–964. [CrossRef]
99. Kim, E.-S.; Oh, J.-S. High-Efficiency Bidirectional LLC Resonant Converter with Primary Auxiliary Windings. *Energies* **2019**, *12*, 4692. [CrossRef]
100. Hua, C.C.; Deng, Y.L. A Novel Dual-Bridge LLC Resonant Converter with Wide Range of Low Input Voltage. *Energy Procedia* **2019**, *156*, 361–365. [CrossRef]
101. Jiang, T.; Zhang, J.; Wu, X.; Sheng, K.; Wang, Y. A Bidirectional Three-Level LLC Resonant Converter with PWAM Control. *IEEE Trans. Power Electron.* **2016**, *31*, 2213–2225. [CrossRef]
102. Arazi, M.; Payman, A.; Camara, M.B.; Dakyo, B. Bidirectional Interface Resonant Converter for Wide Voltage Range Storage Applications. *Sustainability* **2022**, *14*, 377. [CrossRef]
103. Xuan, Y.; Yang, X.; Chen, W.; Liu, T.; Hao, X. A Novel Three-Level CLLC Resonant DC-DC Converter for Bidirectional EV Charger in DC Microgrids. *IEEE Trans. Ind. Electron.* **2021**, *68*, 2334–2344. [CrossRef]
104. Jiao, Y.; Jovanovic, M.M. Topology Evaluation and Comparison for Isolated Multilevel DC/DC Converter for Power Cell in Solid State Transformer. In Proceedings of the 2019 IEEE Applied Power Electronics Conference and Exposition (APEC), Anaheim, CA, USA, 17–21 March 2019; pp. 802–809. [CrossRef]
105. Waffler, S.; Kolar, J.W. A Novel Low-Loss Modulation Strategy for High-Power Bi-Directional Buck+Boost Converters. *IEEE Trans. Power Electron.* **2007**, *24*, 889–894. [CrossRef]
106. Ahamed, M.E.; Senthilkumar, S. Review of Bidirectional DC-DC Converters. *Int. J. Adv. Res. Innov.* **2017**, *5*, 33–42. [CrossRef]
107. Song, M.S.; Son, Y.D.; Lee, K.H. Non-Isolated Bidirectional Soft-Switching SEPIC/ZETA Converter with Reduced Ripple Currents. *J. Power Electron.* **2014**, *14*, 649–660. [CrossRef]
108. Institute of Electrical and Electronics Engineers. 2016 2nd International Young Scientists Forum on Applied Physics and Engineering, YSF 2016—Forum Proceedings. In Proceedings of the 2016 II International Young Scientists Forum on Applied Physics and Engineering, Kharkiv, Ukraine, 10–14 October 2016; pp. 22–28.

109. Li, C.; Herrera, L.; Jia, J.; Fu, L.; Isurin, A.; Cook, A.; Huang, Y.; Wang, J. Design and Implementation of a Bidirectional Isolated Ćuk Converter for Low-Voltage and High-Current Automotive DC Source Applications. *IEEE Trans. Veh. Technol.* **2014**, *63*, 2567–2577. [CrossRef]
110. Lee, H.S.; Yun, J.J. High-Efficiency Bidirectional Buck-Boost Converter for Photovoltaic and Energy Storage Systems in a Smart Grid. *IEEE Trans. Power Electron.* **2019**, *34*, 4316–4328. [CrossRef]
111. Zhang, H.; Chen, Y.; Park, S.J.; Kim, D.H. A Family of Bidirectional DC-DC Converters for Battery Storage System with High Voltage Gain. *Energies* **2019**, *12*, 1289. [CrossRef]
112. Vighetti, S.; Ferrieux, J.P.; Lembeye, Y. Optimization and Design of a Cascaded DC/DC Converter Devoted to Grid-Connected Photovoltaic Systems. *IEEE Trans. Power Electron.* **2012**, *27*, 2018–2027. [CrossRef]
113. Mak, O.C.; Ioinovici, A. Switched-Capacitor Inverter with High Power Density and Enhanced Regulation Capability. *IEEE Trans. Circuits Syst. I Fundam. Theory Appl.* **1998**, *45*, 336–347. [CrossRef]
114. Makowski, M.S.; Maksimovic, D. Performance Limits of Switched-Capacitor DC-DC Converters. *PESC Rec.—IEEE Annu. Power Electron. Spec. Conf.* **1995**, *2*, 1215–1221. [CrossRef]
115. Barzegarkhoo, R.; Forouzesh, M.; Lee, S.S.; Blaabjerg, F.; Siwakoti, Y.P. Switched-Capacitor Multilevel Inverters: A Comprehensive Review. *IEEE Trans. Power Electron.* **2022**, *37*, 11209–11243. [CrossRef]
116. Thiyagarajan, A.; Praveen Kumar, S.G.; Nandini, A. Analysis and Comparison of Conventional and Interleaved DC/DC Boost Converter. In Proceedings of the Second International Conference on Current Trends in Engineering and Technology—ICCTET 2014, Coimbatore, India, 8 July 2014; pp. 198–205. [CrossRef]
117. Zhao, B.; Song, Q.; Liu, W.; Sun, Y. Overview of Dual-Active-Bridge Isolated Bidirectional DC-DC Converter for High-Frequency-Link Power-Conversion System. *IEEE Trans. Power Electron.* **2014**, *29*, 4091–4106. [CrossRef]
118. Henao-Bravo, E.E.; Ramos-Paja, C.A.; Saavedra-Montes, A.J.; González-Montoya, D.; Sierra-Pérez, J. Design Method of Dual Active Bridge Converters for Photovoltaic Systems with High Voltage Gain. *Energies* **2020**, *13*, 1711. [CrossRef]
119. Gorji, S.A.; Sahebi, H.G.; Ektesabi, M.; Rad, A.B. Topologies and Control Schemes of Bidirectional DC–DC Power Converters: An Overview. *IEEE Access* **2019**, *7*, 117997–118019. [CrossRef]
120. Shen, C.L.; Shen, Y.S.; Tsai, C.T. Isolated DC-DC Converter for Bidirectional Power Flow Controlling with Soft-Switching Feature and High Step-up/down Voltage Conversion. *Energies* **2017**, *10*, 296. [CrossRef]
121. Lu, Y.J.; Liang, T.J.; Lin, C.H.; Chen, K.H. Design and Implementation of a Bidirectional DC-DC Forward/Flyback Converter with Leakage Energy Recycled. In Proceedings of the 2017 Asian Conference on Energy, Power and Transportation Electrification (ACEPT), Singapore, 24–26 October 2017; pp. 1–6. [CrossRef]
122. Meng, X.; Zhang, C.; Feng, J.; Kan, Z. Analysis of Soft Switching Conditions for Push-Pull Current Type Bidirectional DC/DC Converter. *IEEE Access* **2024**, *12*, 59386–59398. [CrossRef]
123. Li, S.; Xiangli, K.; Smedley, K.M. A Control Map for a Bidirectional PWM Plus Phase-Shift-Modulated Push-Pull DC-DC Converter. *IEEE Trans. Ind. Electron.* **2017**, *64*, 8514–8524. [CrossRef]
124. Mohammadi, F.; Khorsandi, A. Dual-Input Single-Output High Step-up DC–DC Converter for Renewable Energy Applications. *IET Power Electron.* **2024**, *17*, 337–349. [CrossRef]
125. Banaei, M.R.; Ardi, H.; Alizadeh, R.; Farakhor, A. Non-Isolated Multi-Input-Single-Output DC/DC Converter for Photovoltaic Power Generation Systems. *IET Power Electron.* **2014**, *7*, 2806–2816. [CrossRef]
126. Hou, S.; Chen, J.; Sun, T.; Bi, X. Multi-Input Step-Up Converters Based on the Switched-Diode-Capacitor Voltage Accumulator. *IEEE Trans. Power Electron.* **2016**, *31*, 381–393. [CrossRef]
127. Zhou, L.W.; Zhu, B.X.; Luo, Q.M. High Step-up Converter with Capacity of Multiple Input. *IET Power Electron.* **2012**, *5*, 524–531. [CrossRef]
128. Harini, S.; Chellammal, N.; Chokkalingam, B.; Mihet-Popa, L. A Novel High Gain Dual Input Single Output Z-Quasi Resonant (ZQR) DC/DC Converter for Off-Board EV Charging. *IEEE Access* **2022**, *10*, 83350–83367. [CrossRef]
129. Kumar, G.G.; Sundaramoorthy, K. Dual-Input Non-isolated DC-DC Converter with Vehicle-to-Grid Feature. *IEEE J. Emerg. Sel. Top. Power Electron.* **2022**, *10*, 3324–3336. [CrossRef]
130. Zhou, Z.; Wu, H.; Ma, X.; Xing, Y. A Non-Isolated Three-Port Converter for Stand-Alone Renewable Power System. *IECON Proc. (Ind. Electron. Conf.)* **2012**, *3*, 3352–3357. [CrossRef]
131. Deihimi, A.; Seyed Mahmoodieh, M.E.; Iravani, R. A New Multi-Input Step-up DC–DC Converter for Hybrid Energy Systems. *Electr. Power Syst. Res.* **2017**, *149*, 111–124. [CrossRef]
132. Varesi, K.; Hosseini, S.H.; Sabahi, M.; Babaei, E. A High-Voltage Gain Non-isolated Noncoupled Inductor Based Multi-Input DC-DC Topology with Reduced Number of Components for Renewable Energy Systems. *Int. J. Circuit Theory Appl.* **2018**, *46*, 505–518. [CrossRef]
133. Zhu, B.; Zeng, Q.; Chen, Y.; Zhao, Y.; Liu, S. A Dual-Input High Step-Up DC/DC Converter with ZVT Auxiliary Circuit. *IEEE Trans. Energy Convers.* **2019**, *34*, 161–169. [CrossRef]
134. Chen, Y.M.; Liu, Y.C.; Lin, S.H. Double-Input PWM DC/DC Converter for High-/Low-Voltage Sources. *IEEE Trans. Ind. Electron.* **2006**, *53*, 1538–1545. [CrossRef]
135. Ferreira, A.d.O.; Brito, A.U.; Galhardo, M.A.B.; Ferreira, L.; Macêdo, W.N. Modeling, Control and Simulation of a Small Photovoltaic-Wind Water Pumping System without Battery Bank. *Comput. Electr. Eng.* **2020**, *84*, 106619. [CrossRef]

136. Hassan, Z.; Khan, M.A.; Islam, M.R. Advanced DC-DC Converter Topologies to Boost the Voltage Gain for High Voltage Applications. *Clean Energy* **2024**, *7*, 555–570.
137. Zhou, G.; Tian, Q.; Wang, L. Soft-Switching High Gain Three-Port Converter Based on Coupled Inductor for Renewable Energy System Applications. *IEEE Trans. Ind. Electron.* **2022**, *69*, 1521–1536. [CrossRef]
138. Zheng, Y.; Brown, B.; Xie, W.; Li, S.; Smedley, K. High Step-Up DC-DC Converter with Zero Voltage Switching and Low Input Current Ripple. *IEEE Trans. Power Electron.* **2020**, *35*, 9418–9431. [CrossRef]
139. Wu, H.; Wong, S.C.; Tse, C.K.; Chen, Q. Control and Modulation of Bidirectional Single-Phase AC-DC Three-Phase-Leg SPWM Converters with Active Power Decoupling and Minimal Storage Capacitance. *IEEE Trans. Power Electron.* **2016**, *31*, 4226–4240. [CrossRef]
140. Yodwong, B.; Guilbert, D.; Phattanasak, M.; Kaewmanee, W.; Hinaje, M.; Vitale, G. AC-DC Converters for Electrolyzer Applications: State of the Art and Future Challenges. *Electronics* **2020**, *9*, 912. [CrossRef]
141. Yaramasu, V.; Dekka, A.; Durán, M.J.; Kouro, S.; Wu, B. PMSG-Based Wind Energy Conversion Systems: Survey on Power Converters and Controls. *IET Electr. Power Appl.* **2017**, *11*, 956–968. [CrossRef]
142. Nejabatkhah, F.; Li, Y.W.; Tian, H. Power Quality Control of Smart Hybrid AC/DC Microgrids: An Overview. *IEEE Access* **2019**, *7*, 52295–52318. [CrossRef]
143. Yaramasu, V.; Wu, B.; Sen, P.C.; Kouro, S.; Narimani, M. High-Power Wind Energy Conversion Systems: State-of-the-Art and Emerging Technologies. *Proc. IEEE* **2015**, *103*, 740–788. [CrossRef]
144. Alili, A.; Camara, M.B.; Dakyo, B.; Raharijaona, J. Reliability and Performances of Power Electronic Converters in Wind Turbine Applications. *Int. J. Adv. Intell. Syst.* **2021**, *14*, 61–72.
145. Kitagawa, W.; Thiringer, T. Inverter Loss Analysis and Comparison for a 5 MW Wind Turbine System. In Proceedings of the 2017 19th European Conference on Power Electronics and Applications (EPE'17 ECCE Europe), Warsaw, Poland, 11–14 September 2017; pp. 1–10. [CrossRef]
146. Flourentzou, N.; Agelidis, V.G.; Demetriades, G.D. VSC-Based HVDC Power Transmission Systems: An Overview. *IEEE Trans. Power Electron.* **2009**, *24*, 592–602. [CrossRef]
147. Blaabjerg, F.; Ma, K.; Yang, Y. Power Electronics for Renewable Energy Systems—Status and Trends. In Proceedings of the CIPS 2014 8th International Conference on Integrated Power Electronics Systems, Nuremberg, Germany, 25–27 February 2014; VDE: Nuremberg, Germany, 2014.
148. Blaabjerg, F.; Ma, K. Future on Power Electronics for Wind Turbine Systems. *IEEE J. Emerg. Sel. Top. Power Electron.* **2013**, *1*, 139–152. [CrossRef]
149. Lingom, P.M.; Song-Manguelle, J.; Nyobe-Yome, J.M.; Doumbia, M.L. A Comprehensive Review of Compensation Control Techniques Suitable for Cascaded H-Bridge Multilevel Inverter Operation with Unequal DC Sources or Faulty Cells. *Energies* **2024**, *17*, 722. [CrossRef]
150. Gao, D.Z.; Sun, K. Chapter 16—DC–AC Inverters. In *Electric Renewable Energy Systems*; Muhammad, H.R., Ed.; Academic Press: Boston, MA, USA, 2016; pp. 354–381, ISBN 978-012804448-3.
151. Samizadeh, M.; Yang, X.; Karami, B.; Chen, W.; Blaabjerg, F.; Kamranian, M. A New Topology of Switched-Capacitor Multilevel Inverter with Eliminating Leakage Current. *IEEE Access* **2020**, *8*, 76951–76965. [CrossRef]
152. Krishna, R.A.; Suresh, L.P. A Brief Review on Multi Level Inverter Topologies. In Proceedings of the 2017 International Conference on Data Management, Analytics and Innovation (ICDMAI), Pune, India, 24–26 February 2017. [CrossRef]
153. Gorla, N.B.Y.; Kolluri, S.; Chai, M.; Panda, S.K. An Open-Circuit Fault Detection and Localization Scheme for Cascaded H-Bridge Multilevel Converter without Additional Sensors. *IEEE Trans. Ind. Appl.* **2021**, *58*, 457–467. [CrossRef]
154. Perra, A. PWM Inverter Technology. *IEEE Aerosp. Electron. Syst. Mag.* **1992**, *7*, 20–22. [CrossRef]
155. Klug, R.D.; Klaassen, N. High Power Medium Voltage Drives—Innovations, Portfolio, Trends. In Proceedings of the 2005 European Conference on Power Electronics and Applications, Dresden, Germany, 11–14 September 2005. [CrossRef]
156. José, R.; Franquelo, L.G.; Samir, K.; León, J.I.; Portillo, R.C.; Prats, M.Á.M.; Pérez, M.A. Multilevel Converters: An Enabling Technology for High-Power Applications. *Proc. IEEE* **2009**, *97*, 1786–1817. [CrossRef]
157. Franquelo, L.G.; Rodriguez, J.; Leon, J.I.; Kouro, S.; Portillo, R.; Prats, M.A.M. The Age of Multilevel Converters Arrives. *IEEE Ind. Electron. Mag.* **2008**, *2*, 28–39. [CrossRef]
158. Khoun Jahan, H.; Abapour, M.; Zare, K. Switched-Capacitor-Based Single-Source Cascaded H-Bridge Multilevel Inverter Featuring Boosting Ability. *IEEE Trans. Power Electron.* **2019**, *34*, 1113–1124. [CrossRef]
159. Kumari, S.; Verma, A.; Sandeep, N.; Yaragatti, U.; Pota, H. A Five-Level Transformer-Less Inverter with Self-Voltage Balancing and Boosting Ability. *IEEE Trans. Ind. Appl.* **2021**, *57*, 6237–6245. [CrossRef]
160. Menye, J.S.; Lingom, P.M.; Song-Manguelle, J.; Nyobe-Yome, J.M.; Doumbia, M.L. Effects of Control Strategies on the Assessment of Power Converter Losses in Electric Vehicle Drivetrains. In Proceedings of the 2023 IEEE Canadian Conference on Electrical and Computer Engineering (CCECE), Regina, SK, Canada, 24–27 September 2023; pp. 235–241.
161. Lam, C.-S.; Wong, M.-C.; Han, Y.-D. Hysteresis Current Control of Hybrid Active Power Filters. *IET Power Electron.* **2012**, *5*, 1175–1187. [CrossRef]
162. Singh, J.K.; Behera, R.K. Hysteresis Current Controllers for Grid Connected Inverter: Review and Experimental Implementation. In Proceedings of the 2018 IEEE International Conference on Power Electronics, Drives and Energy Systems (PEDES), Chennai, India, 18–21 December 2018; pp. 1–6.

163. Holmes, D.G.; Lipo, T.A. *Pulse Width Modulation for Power Converters: Principles and Practice*; John Wiley and Sons: Hoboken, NJ, USA, 2003; Volume 18.
164. Antonio-Ferreira, A.; Collados-Rodriguez, C.; Gomis-Bellmunt, O. Modulation Techniques Applied to Medium Voltage Modular Multilevel Converters for Renewable Energy Integration: A Review. *Electr. Power Syst. Res.* **2018**, *155*, 21–39. [CrossRef]
165. Holtz, J.; Lotzkat, W.; Werner, K.-H. A High-Power Multitransistor-Inverter Uninterruptable Power Supply System. *IEEE Trans. Power Electron.* **1988**, *3*, 278–285. [CrossRef]
166. Agelidis, V.G.; Calais, M. Application Specific Harmonic Performance Evaluation of Multicarrier PWM Techniques. In Proceedings of the PESC 98 Record. 29th Annual IEEE Power Electronics Specialists Conference (Cat. No. 98CH36196), Fukuoka, Japan, 22 May 1998; Volume 1, pp. 172–178.
167. Wu, B.; Narimani, M. *High-Power Converters and AC Drives*; John Wiley & Sons: Hoboken, NJ, USA, 2017.
168. Bushra, E.; Zeb, K.; Ahmad, I.; Khalid, M. A Comprehensive Review on Recent Trends and Future Prospects of PWM Techniques for Harmonic Suppression in Renewable Energies Based Power Converters. *Results Eng.* **2024**, *22*, 102213. [CrossRef]
169. Lin, H.; Cai, C.; Chen, J.; Gao, Y.; Vazquez, S.; Li, Y. Modulation and Control Independent Dead-Zone Compensation for H-Bridge Converters: A Simplified Digital Logic Scheme. *IEEE Trans. Ind. Electron.* **2024**, *71*, 15239–15244. [CrossRef]
170. Jayakumar, V.; Chokkalingam, B.; Munda, J.L. A Comprehensive Review on Space Vector Modulation Techniques for Neutral Point Clamped Multi-Level Inverters. *IEEE Access* **2021**, *9*, 112104–112144. [CrossRef]
171. Lingom, P.M.; Song-Manguelle, J.; Menye, J.; Unruh, R.; Doumbia, M.L.; Jin, T. A Single-Carrier PWM Method for Uniform Step Asymmetrical Multilevel Converters. In Proceedings of the 2023 IEEE Energy Conversion Congress and Exposition (ECCE), Nashville, TN, USA, 29 October–2 November 2023; pp. 3599–3606.
172. Xie, D.; Lin, C.; Deng, Q.; Lin, H.; Cai, C.; Basler, T.; Ge, X. Simple Vector Calculation and Constraint-Based Fault-Tolerant Control for a Single-Phase CHBMC. *IEEE Trans. Power Electron.* **2024**. [CrossRef]
173. Ogata, K. *Modern Control Engineering*, 5th ed.; Pearson Education: Upper Saddle River, NJ, USA, 2010.
174. Lin, H.; Chung, H.S.-H.; Shen, R.; Xiang, Y. Enhancing Stability of Dc Cascaded Systems with CPLs Using MPC Combined with NI and Accounting for Parameter Uncertainties. *IEEE Trans. Power Electron.* **2024**, *39*, 5225–5238. [CrossRef]
175. Xu, Q.; Yan, Y.; Zhang, C.; Dragicevic, T.; Blaabjerg, F. An Offset-Free Composite Model Predictive Control Strategy for DC/DC Buck Converter Feeding Constant Power Loads. *IEEE Trans. Power Electron.* **2019**, *35*, 5331–5342. [CrossRef]
176. Boukhnifer, M.; Chaibet, A.; Larouci, C. Experimental H-Infinity Robust Control of Aerial Vehicle Flight. In Proceedings of the 2011 19th Mediterranean Conference on Control & Automation (MED), Corfu, Greece, 20–23 June 2011; pp. 242–247.
177. Toure, I.; Camara, M.-B.; Dakyo, B. Literature Review Based Control Strategies of Electrolyzers Systems. In Proceedings of the 2024 12th International Conference on Smart Grid (icSmartGrid), Shanghai, China, 25–27 October 2024; pp. 155–161.
178. Babaiahgari, B.; Jeong, Y.; Park, J.-D. Dynamic Control of Region of Attraction Using Variable Inductor for Stabilizing DC Microgrids with Constant Power Loads. *IEEE Trans. Ind. Electron.* **2020**, *68*, 10218–10228. [CrossRef]
179. Mosayebi, M.; Sadeghzadeh, S.M.; Gheisarnejad, M.; Khooban, M.H. Intelligent and Fast Model-Free Sliding Mode Control for Shipboard DC Microgrids. *IEEE Trans. Transp. Electrif.* **2020**, *7*, 1662–1671. [CrossRef]